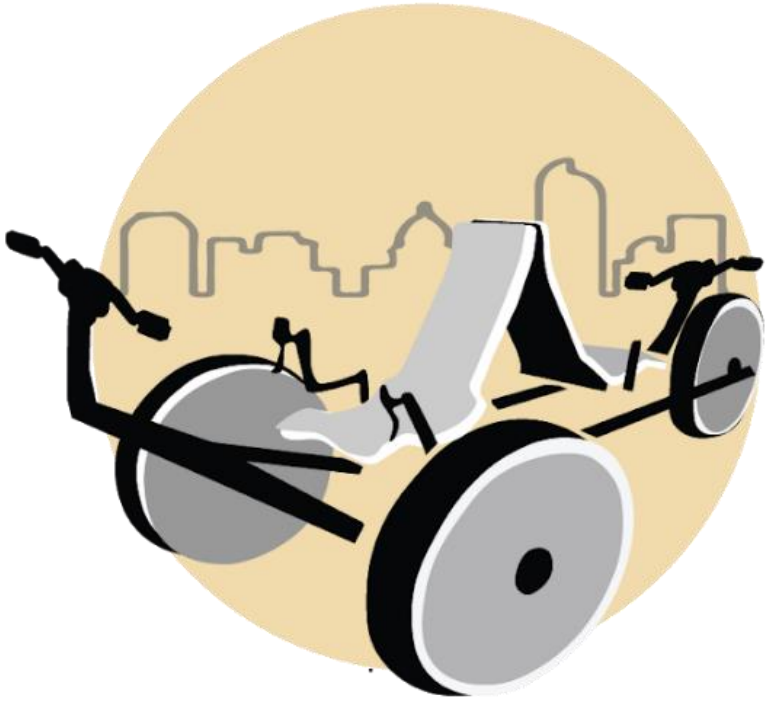

NASA Human Exploration Rover

May 5, 2020

Denver Endeavour Team:

Feras Alfaresi, James Catlin, Madison Gast, Taisiya Lushnikova, Faith Martin, Kolton Munson, and Daniel Tomlin

Abstract

The Denver Endeavour Rover team is a continuation of the Rover project at the University of Colorado Denver. Annually, NASA hosts its Human Exploration Rover Challenge in Huntsville, Alabama for International collegiate and high school teams to put their rover designs to the test. Denver Endeavour seeks to place first in the competition and win the Neil Armstrong Best Design Award for having the best technical approach and best-engineered design for extraterrestrial terrain. A virtual award ceremony for the NASA competition will be held in late May.

This year, the Denver Endeavour team focused on updating the steering system, wheels design, and frame design, of the previous rover to enhance its abilities on the competition course. The steering on the Endeavour was redesigned to correct complications made when torsion caused the steering to seize. The previous linear steering has been redesigned using parallelogram-like pitman linkages with corrected Ackermann geometry, which converts equal forward and backward linear motion at the handles to rotational motion at the pitman arm, turning the wheels. This new system is isolated from the rest of the rover frame in order to minimize torsion effects, seen from the previous team. The Denver Endeavour team redesigned and manufactured the wheels to reduce weight and decrease the chances of deformation while completing obstacles on the course. The wheels were designed as hollow, conical, carbon fiber shells, that housed a central aluminum wheel hub. The conical design allowed for the removal of internal supports and prevented the wheel from shifting laterally, thus reducing the stress on the carbon fiber shell. In addition, the new wheels were 25% lighter than the previous design. This year, the Endeavour included a custom hinge on the front pedal post, which allowed for the rover

to fit within a 5’x5’x5’ cube, as specified by NASA. This hinge allows the front pedals to fold inward toward the seat, shortening the overall length of the vehicle by 9 inches.

At the present time, the Denver Endeavour team has been selected as one of the top finalists for the Neil Armstrong Best Design Award and is eagerly awaiting additional contact from NASA, regarding the awards ceremony, and we hope to bring a victory home to University of Colorado Denver.

Table of Contents

List of Figures

Introduction

NASA is currently in the process of sending astronauts back to the Moon by 2024, including the first woman to step foot on this landscape. Once on the Lunar surface, rovers provide a much-needed extension to the astronaut's capabilities while exploring and experimenting. Every Spring, NASA hosts its annual Human Exploration Rover Challenge in Huntsville, Alabama to challenge teams from around the world to engineer rovers to be used for completing tasks on extraterrestrial terrains. The Denver Endeavour team from the University of Colorado Denver will be competing this upcoming April.

This competition utilizes a point system, where the team with the most points will win. Points can be obtained by completing tasks and obstacles along the half-mile course, or by having certain design elements integrated into the team's rover. Due to space travel limitations, NASA encourages the rover designs to be both lightweight and compact, rewarding teams with more points for these categories. The rovers are to be designed to fit within a 5'x5'x5' volume cube and weigh less than 210 pounds. In addition, all the rovers must be powered by the passengers, meaning no motors or anything that would increase the kinetic energy output.

On the first day of competition, each team's rover must complete the Mission Readiness Review (MRR) that will check for proper volume and clearance constraints, weight, and the folding/unfolding assembly. Then, before each course run, each rover is inspected during an Excursion Readiness Review (ERR) to ensure National flags are present and visible, and that all safety requirements have been met. On the course, there are a total of 14 obstacles and five tasks available for each team to complete within an eight-minute timeframe. Obstacles vary in difficulty and include the following:

1. Undulating Terrain - ramps ranging from 6 to 12 inches in height with gradual ingress and egress slopes, all covered with gravel
2. Crater with Ejecta - large crater 3 feet in diameter and 8 inches in height, covered with gravel
3. Side Incline - 20-degree incline perpendicular to the direction of rover traverse
4. High Butte - butte 5 feet high with a 20-degree incline
5. Large Ravine - 2-foot depression, about 8 feet wide
6. Martian Sand Dunes - dunes about 2 feet high and 3 feet wide at the base
7. Crevasses - vary in width between 1 and 4 inches and 4 to 6 inches deep
8. Ice Geyser Slalom - navigating downhill, avoiding contact with geysers
9. Lunar Crater - asphalt lava with craters of various sizes and strewn boulders testing the 12-inch clearance of the vehicle
10. Bouldering Rocks - asteroid debris (boulders) ranging in size from 3 to 12 inches
11. Tilted Craters - medium craters on downslope of 15 degrees
12. Loose Regolith - sand pit 6 to 8 inches in depth
13. Pea Gravel - small rounded pebbles deposited to a depth of about 6 inches
14. Undulating Hills - hills randomly positioned so that they occur first on one side of the rover, then on the other, producing twisting forces on the chassis

Eleven of the above-mentioned obstacles have bypass options. The five tasks on the course include three sample collection tasks, one stereographic analysis task, and one instrument deployment task which cannot be skipped.

In addition to the point system for the competition, awards are given to teams that meet specific criteria. Of these awards, previous teams from University of Colorado Denver have received both the Neil Armstrong Best Design Award and the Featherweight Award. The Featherweight Award is given to the team whose rover is the lightest weight and meets the following two requirements: must complete the course in under eight minutes and must accumulate at least 40 points in a single run. The Neil Armstrong Best Design Award is given to the team whose rover is deemed the best engineered design for navigating the extraterrestrial terrain and it is based not only on rover performance, but also the technical approach taken by the team. In addition to these two awards, first, second, and third place podium awards are given to teams based on total points, along with 11 other awards for best report, telemetry, drivetrain, system safety, most improved, crash and burn, team spirit, pit crew awards, wheel design and technology, STEM engagement, and rookies. Our Denver Endeavour Team is determined to have a 1st place finish and win the Neil Armstrong Best Design Award.

Rider Selection

Introduction

It was important for the Endeavour team to determine the two riders early because we needed information regarding the weight of the rover, as well as, the total combined weight of the rover with the riders, in order to properly run analysis on certain components. In addition, the riders needed to be chosen because the heights of each rider are important in determining

the necessary added length to the rear crank post design, as well as, the positions of both the front and rear seat.

Wellness Center Testing

In order to determine which team members would be the two chosen to power the Endeavour during competition, our team completed testing at the CU Denver Student Wellness Center. Initially, we used the recumbent bikes over a longer riding period to determine each rider's average power output, but soon determined that this data was ineffective in determining the best riders. To combat this issue, we decided to perform a second round of testing for each rider. This second round of testing was performed by having each rider maintain a specified RPM. Each rider increased resistance, as long as they continued to maintain the specified RPM. Once the resistance was increased to a point where the RPM was no longer maintained, it was lowered by one, and the power output, at this maintainable resistance, was recorded. Each rider had a different resistance level, but the RPM allowed for a comparable control in the testing. The following RPMs were maintained by each rider during testing: 70, 80, 90, and 100. This range from 70 to 100 RPM was chosen because the natural cadence for most cyclists is located within this range. The power outputs recorded from the recumbent bicycles was recorded in Watts and called the "Instantaneous Power". The results from this testing can be seen in *Table 1* below. Another goal of this testing was to also determine the cadence of each rider so the gearing could be adjusted accordingly for competition.

Table 1: Instantaneous power values obtained from recumbent bike testing

RPM:	70	80	90	100
Rider	Instantaneous Power (W)	Instantaneous Power (W)	Instantaneous Power (W)	Instantaneous Power (W)
Dan	206	243	302	353
Faith	107	116	173	214
Feras	208	275	353	388
Maddie	155	190	263	317
Kolton	103	201	296	353
James	125	260	280	246
Taisiya	164	180	300	282
Dylan	315	340	351	388

Power-to-Weight Ratios

Power-to-weight ratios were very important in determining the appropriate riders for competition. Due to the range of weights of our team members, it was expected that the power outputs would also be ranging greatly. In order to normalize this data, we divided out the weight of each rider so the data could be looked at, and compared, side-by-side. This normalization was very insightful and allowed us to make our best decision. This ratio was calculated using the average power in Watts which was the instantaneous power value from 80 RPM for each rider, since 80 RPM was the closest to each rider's cadence. Each rider's weight was converted to Newtons and then divided from the average power value; therefore, the units of the power-to-weight ratio is meters per second, which is equal to our 20° climbing velocity.

20° Incline Climbing Velocity

Each rider's climbing velocity for a 20° incline was calculated using the power-to-weight ratio, as described above, and the geometry of the 20° incline. *Figure 1* shows the relationship between the incline and the rover.

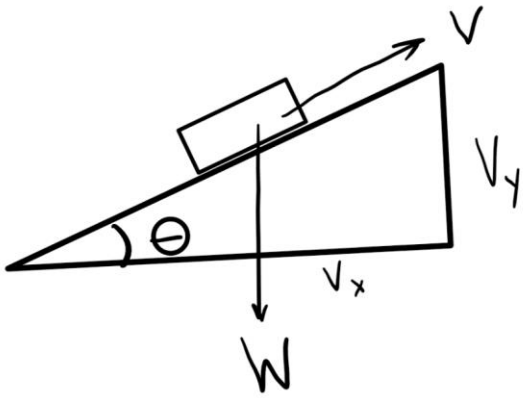

Figure 1: Free body diagram showing the rover accelerating on an incline

In *Figure 1*, *W* is the weight of the rover and rider together, *V* is the velocity of the rover uphill, *Θ* is the angle of the incline, and V_x and V_y are the horizontal and vertical velocities, respectively. *Equation 1* was used to determine the vertical climbing velocity for each rider.

$$Power = FV = WV\sin(\theta) \quad (1)$$

Where *F* is the vertical force on the rover, *V* is the velocity along the incline, *W* is the combined weight of the rover and rider, and θ is the angle of incline. By rearranging *Equation 1* to utilize the power-to-weight ratio, we can determine the vertical climbing velocity as seen in *Equation 2*, below.

$$PW = V\,sin(\theta) \quad (2)$$

Where $V\ sin(\theta)$ is the vertical climbing velocity. This vertical climbing velocity helped us to determine the most appropriate rider for the competition. The tabulated results can be seen below in *Table 2*.

Table 2: Results of each rider's climbing velocity and power-to-weight ratio

Rider	Avg Power (Watts)	Weight (lbs)	Weight of Rider (N)	Weight of Rover + Rider (N)	Power to weight Ratio (m/s)	Climbing Velocity (mph)
Dan	243	158	702.8188	1414.53396	0.17179	0.3843
Faith	116	118	524.8900	1236.60516	0.09381	0.2098
Feras	275	152	676.1294	1387.84464	0.19815	0.4432
Maddie	190	200	889.6440	1601.35920	0.11865	0.2654
Kolton	201	194	862.9547	1574.66988	0.12765	0.2855
James	260	221	983.0566	1694.77182	0.15341	0.3432
Dylan	340	242	1076.4692	1788.18444	0.19014	0.4253
Taisiya	180	189	840.7136	1552.42878	0.11595	0.2594

Final Results

The final results of this testing have determined that Feras and Madison are the most suited riders for the competition, due to their high power-to-weight ratios and their faster vertical climbing velocities. In order to maximize each rider's performance, the pedals and seats will have to be adjusted accordingly for each rider. In addition, it was determined that the heavier rider would need to sit at the rear of the rover in order to increase traction during hill climbs.

Endeavour Wheels

Wheels Design

The Denver Endeavour wheels sub-team sought to reduce the maximum weight of each wheel, and to restructure the wheel carcass geometry to reduce the chances of deformation during the competition under different loading. Minor changes will be made to the hub designed by the Odyssey team in 2018, in order to accommodate our new geometry. The overall design of the complete wheel featured an outer ring of tread, made from Polyurethane rubber, with an outer diameter of 27in, overlaying a polyurethane soft foam layer that has a 1in thickness. These

Polyurethane layers will be bonded together, then the foam will be bonded to the wheel carcasses, composed of multiple layers of carbon fiber, which will nest inside one another. The full assembly of the wheel can be seen in *Figure 2 and 3.*

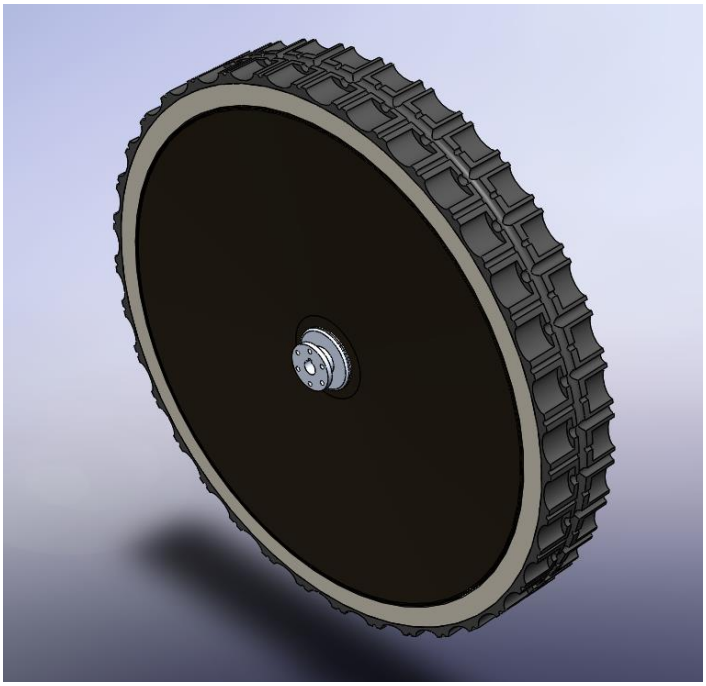

Figure 2: SolidWorks rendering of full-wheel assembly

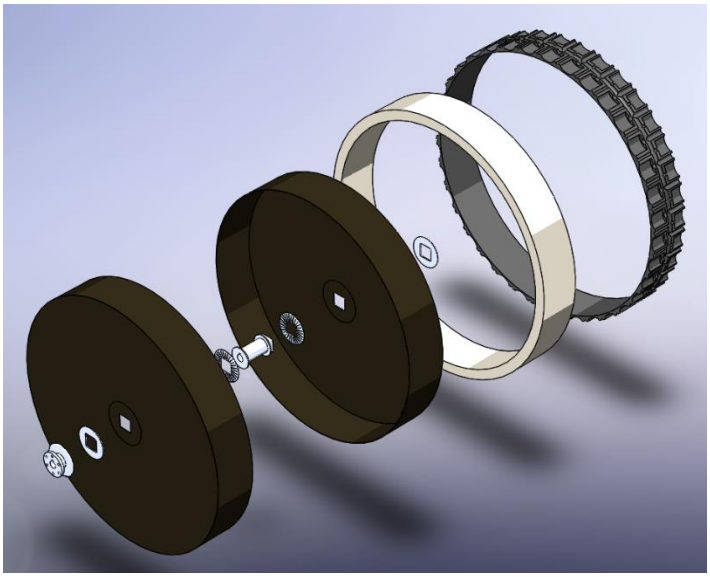

Figure 3: Exploded view of the full wheel assembly

The tread thickness at the point of contact with the ground will be 4in. At the center hub, the sidewalls of the wheel carcasses will have a width of 3in, reducing the width of the Odyssey hub by 1in. The geometry of this side wall has two planes, one plane where the outer ring edge is located and a second plane, 0.5in inward from the outer ring plane, where the hub will pass through. The shape of the sidewall is conical from the inner hub plane to the outer ring plane. This geometry can be seen in *Figure 4,* where plane *A* is the inner hub plane and plane *B* is the outer ring plane.

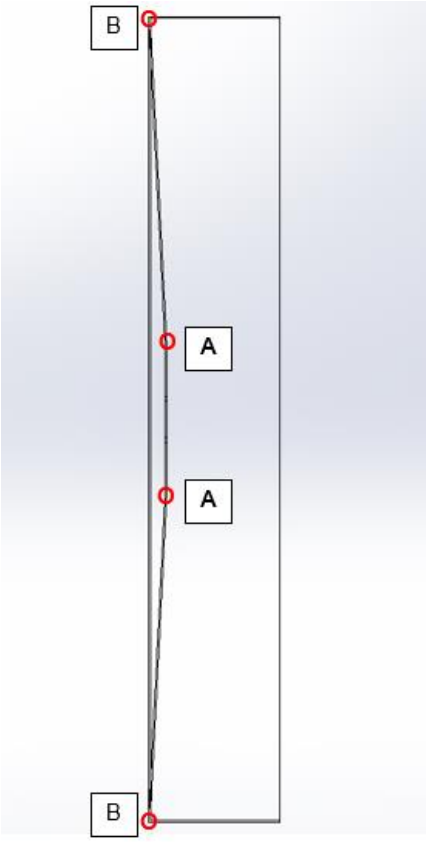

Figure 4: Right side view of the wheel carcass, where red circles indicate edges of planes A and B

A secondary benefit of reducing the center hub width, will be an added clearance for brakes, drivetrain, and steering components.

The overall design of the Odyssey wheels results in a maximum weight of 15 lbs and our goal is to reduce this to 10 lbs. Reducing the maximum weight of each wheel by 5 lbs will result in a 15 lb weight reduction of the whole vehicle. Weight has also been saved in the hub by reducing the center section width by 1in, and the reinforcement disks were reduced from a previous diameter of 4in to a new diameter of 3in. The full updated assembly of the center hub is seen in *Figure 5.* The wheel carcasses will have opposite orientations, openings facing each other, and the brake side carcass will be placed within the bolt side carcass. Both carcasses will have the circular reinforcement disks adhered to both the inner and outer sides and *Figure 6* shows where the carcasses will be attached in the assembly.

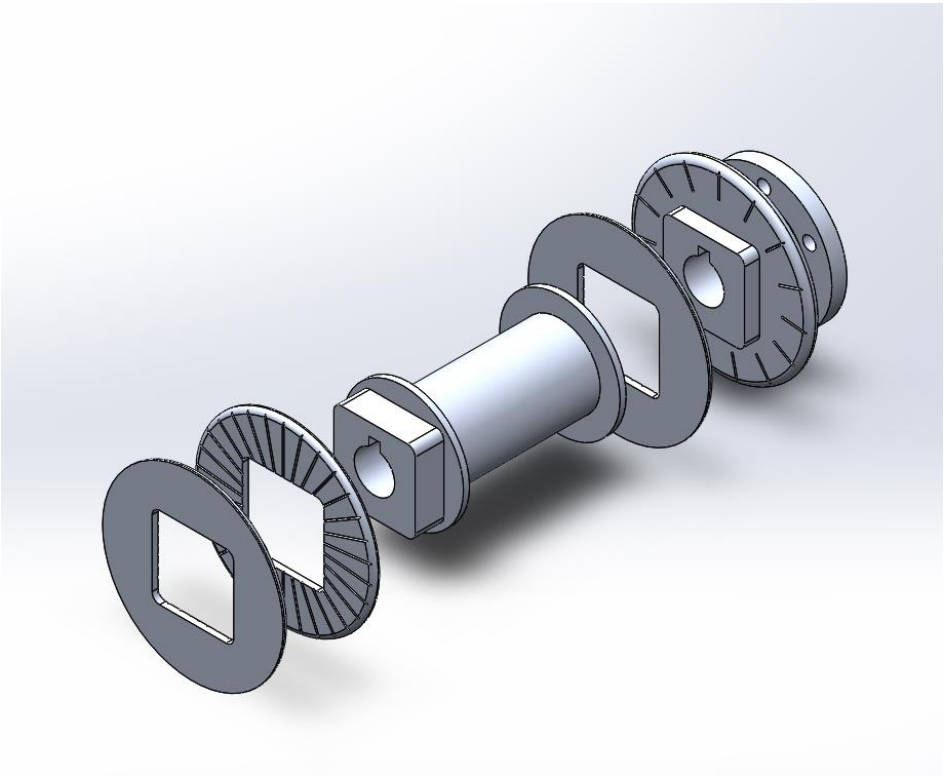

Figure 5: Exploded View of complete wheel hub assembly

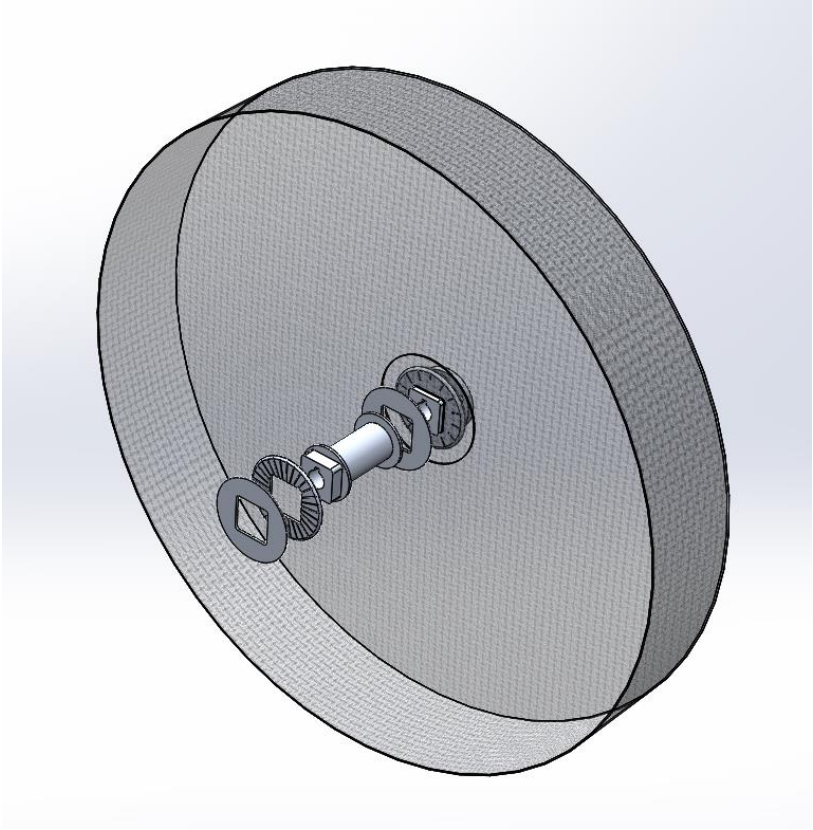

Figure 6: Wheel hub assembly with the inclusion of one wheel carcass

The Odyssey team added reinforcement u-channels to the rear wheel due to the added stress during the competition, specifically during the turns and inclines, due to the change in geometry of our wheels. We will not need to add u-channel supports. We are going to use a 0, 45, 90, 45, 0 degree layup orientation on our wheel carcasses, but we are still needing to run coupon testing to determine the cloth's exact properties and see if the table values for the T300, match the property values we obtain for our carbon fiber. We have determined that we are not in need of as many concentric layers as the Odyssey team used on their sidewalls. The Odyssey team used the following concentric sizes when laying up their carbon fiber: 10in, 12in, 14in, 22in, 23in, 24in, and 26in. We have determined that our design does not require 7 layers and we will

be using 5 layers, instead. The Endeavour sidewall will consist of the following concentric layers: 8in, 14in, 22in, 24in, and 26in. Using a 5-layer design will aid in the 0, 45, 90, 45, 0-degree layup process and make it easier to determine which layers need the orientation.

Analysis and Testing

The riders that will be on the Endeavour during competition have been determined and we have been able to use their combined weight to analyze and test components for the wheels and the wheel hub. The riders chosen are Madison and Feras and their combined weight is 352lbs. There were limitations on the finite element analysis that we were able to run on the computer, on SolidWorks, specifically. MATLAB was used to perform hand calculations while an analysis in Abaqus is worked on. The carbon fiber wheel carcasses were designed to have the sidewalls at a slight angle, as seen previously in *Figure 4*. The angles are 2.89 and 2.93 degrees for the brake side and bolt side shells, respectively. The Odyssey team's m-files *Appendix D-F* were modified to account for Endeavour's new vehicle weight, as well as, the sidewall angle. Using a safety factor of 2, the minimum sidewall thickness for the Endeavour wheels was determined to be 0.03662in instead of the 0.03657in minimum sidewall thickness required with a vertical sidewall. The hoop stress m-file *Appendix D* was modified to reflect Endeavour design changes and the minimum wheel hoop thickness required was calculated to be 0.00457 inches. The bending moment at the hub was recalculated for the new Endeavour design and the safety factor was determined to be 116.

Abaqus and SolidWorks are created by the same company, and it would be convenient if they interoperated nicely with each other, however when we attempted to import the wheel assemblies from SolidWorks to Abaqus, the licenses available to the student lab computers do not have a workable file format in common to both programs. We tried using a third-party program called ParaSolid, with Dr. Carpenter's help, to act as a go between. The ParaSolid program was able to read the SolidWorks file types, but since it was voxel-based, and the wheel shells were so thin artifacts (voids in the hoop section) were observed in the model. After tweaking the two-shell design and redesigning as one combined shell, since we plan on gluing the two shells together, a second import was attempted via ParaSolid, this time, a model was created that was 22 GB and took several hours to accomplish. After several adjustments to settings and switching to hexa-elements instead of tetrahedrons, and more hours, the file for the shell was reduced to 1.8 GB and 11 million elements. Dr. Carpenter was very gracious helping us, but at some point, figuring out Abaqus seemed like the better option. With the hoop stress, sidewall thickness, and hub bending calculations from MATLAB, our main concern for FEA on the wheel carcasses is to gain some insight into the stress concentration, where the sidewall bends into the hoop and it would be nice to see FEA confirmations of the calculations.

The hub analysis has been completed using SolidWorks. When analyzing the hubs, we modified a MATLAB script *Appendix I* from the Odyssey team that calculates the maximum breaking force on each wheel. We then used this maximum braking force as the maximum force, applied as a torsion, to the axle and hub assembly. In order to accomplish a safety factor of 2, we determined if the hub would be able to withstand twice the maximum braking force which was

equal to 7440 in-lbf. The analysis completed on the hub design yielded a minimum safety factor of 6.23.

Wheel Mold Design and Manufacturing

The wheel molds were manufactured using medium density fiberboard (MDF), wood glue, and the ShopBot. MDF board was purchased in 8ft by 4ft sheets and were cut to a more manageable, 30in by 30in, size. Once 12 uniform sized squares of MDF were cut, the boards were glued together in threes. The molds were redesigned from the previous semester's design due to increased limitations with the ShopBot. Due to the limited retract height of the tool on the ShopBot, the original design of a 4-layer half-mold was changed to a 3-layer design. In addition to this change, the original 4-piece design was changed to a 2-piece design with a draft angle of 1.5 degrees. This allowed for simpler molds and reduced the amount of cutting time spent on the ShopBot.

When gluing the 3 layers of MDF together, for the lower half of each mold, or the "base" as it was denoted during design, the bottom two layers of MDF were glued across the entire 30" x 30" surface, while the top board was only glued in the region outside of the wheel diameter, as seen in *Figure 7*.

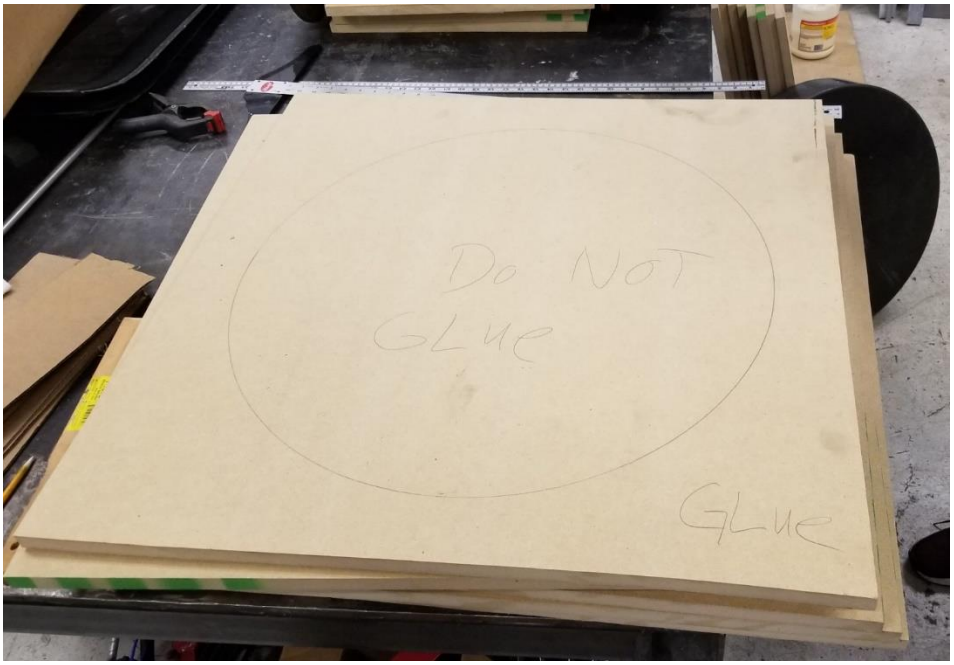

Figure 7: MDF boards with glue pattern for lower mold half

The reason for this glue pattern was to allow the top board to be pried off, after the initial contour of the inner circle, allowing for over an hour of saving machining time. The top half of each mold, or the “upper”, was fully glued between all three layers, since the ShopBot was only performing basic contours. *Figure 8* shows the process of spreading glue across the full surface of the MDF for full adhesion.

Figure 8: Using squeegee spreaders to spread glue evenly across board surface

After all things were glued, the three layers of MDF were clamped and weighted, to prevent any air pockets for 24 hours, as seen in *Figures 9* and *10*.

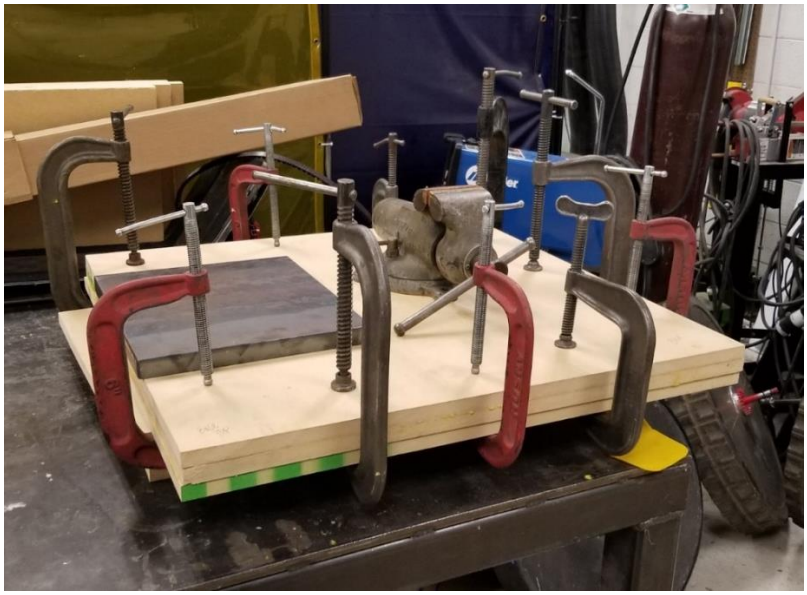

Figure 9: MDF mold clamped on table and weighted at center

Figure 10: 2nd MDF mold clamped to welding table and weighted at center

Once removed from the clamps, the ShopBot process began. Fusion360 was used to create the CAM programming for the ShopBot. For the uppers, 2D contours with a flat endmill were used to remove excess material from the outer edges of each part to create a 28” x 28” tool. In addition to the outer contour, the flat endmill was used to create a 2D contour of the wheel diameter, as seen below in *Figure 11*.

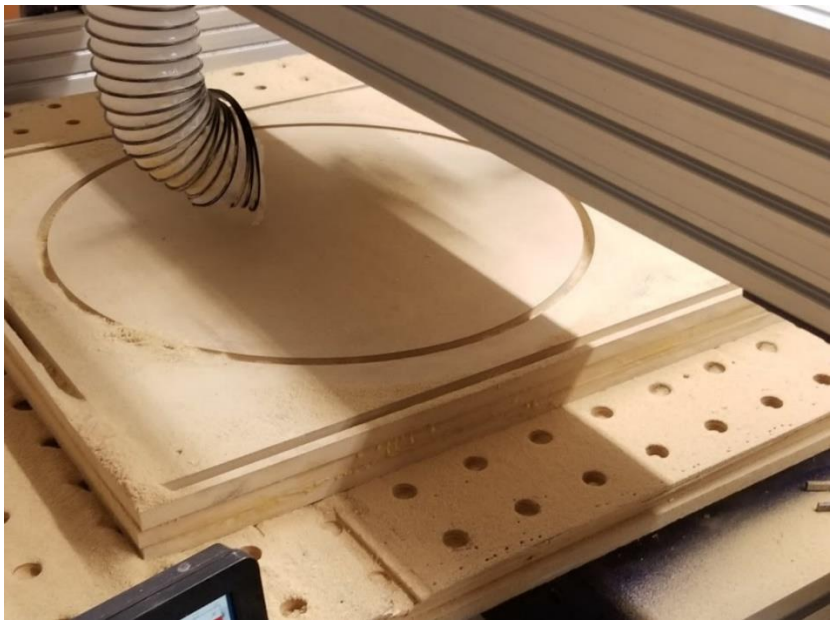

Figure 11: 2D contours of diameter and outer edge of mold

Once these two 2D contours were completed, the inner scrap MDF was removed and can be seen in *Figure 12.*

Figure 12: Inner scrap layers of MDF removed, while ShopBot continued the mill the draft angle

The ball endmill was used to finish the draft angle utilizing smaller stepovers. For the two bases, the same outer and inner 2D contour programs were used. After the inner 2D contour was completed, the top layer of the 3 boards of MDF was removed using a pry bar in order to cut down on the total machining time when running the adaptive clearing on the center, bowl-like portion. After the removal of this board from the center, an adaptive clearing was run to remove the bulk of the material before switching to the ball endmill. The ball endmill completed the part using a parallel function. The adaptive clearing and parallel functions can be seen in *Figures 13, 14 & 15.*

Figure 13: The end result of the adaptive clear function on the ShopBot

Figure 14: Another view of the result of the adaptive clear

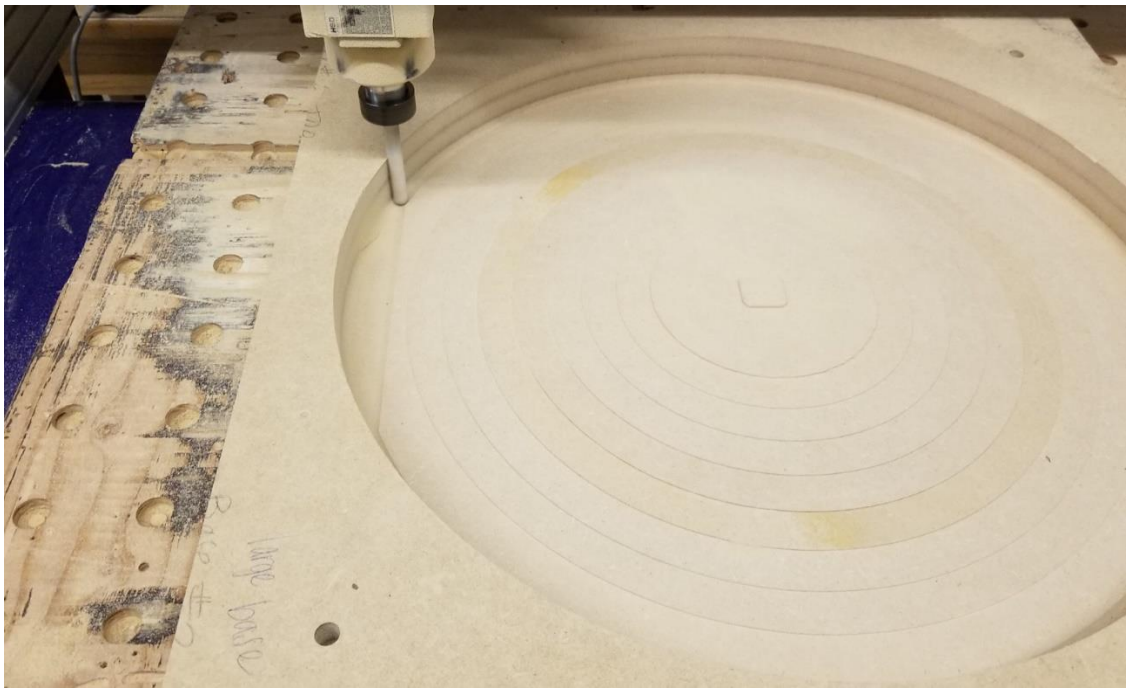

Figure 15: The start of the parallel function run on the ShopBot

An error occurred when the base of the larger mold was being machined with the ball endmill. During the parallel function, the tool slipped out of the collet and cut into the side of the mold, seen in *Figure 16.*

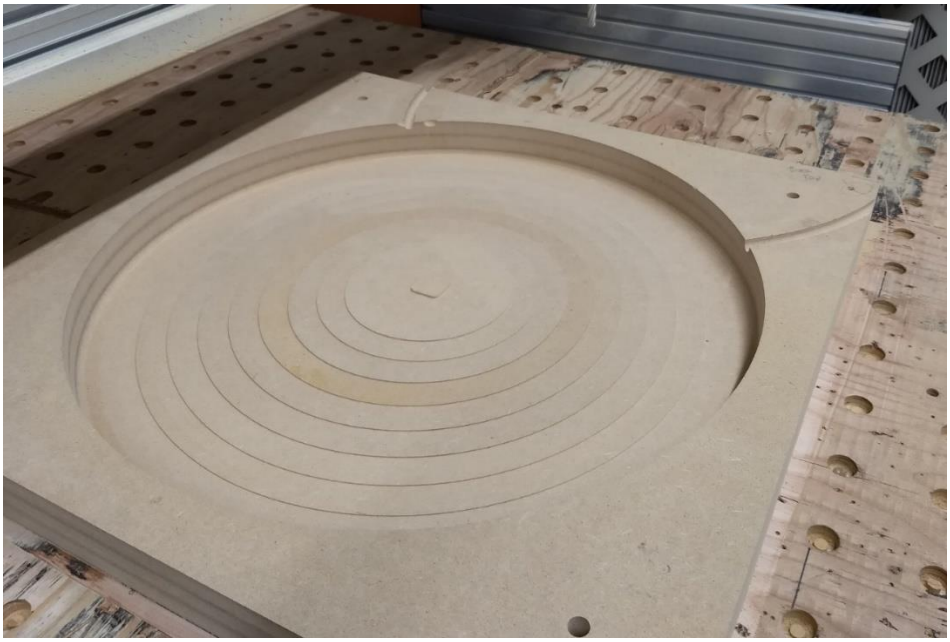

Figure 16: Visible cuts in the far side of the mold, caused by a slipping of the tool within the collet

When the tool was tightened, the ball endmill program was rerun and it ended up cutting completely through the mold, as seen in *Figure 17.* This base portion needed to be remanufactured.

Figure 17: Failure of the first MDF mold

After completing both the uppers and bases on the ShopBot, each upper and base for the larger and smaller molds, respectively, were paired and glued together to create the full mold for each wheel half. Pin holes were drilled on both the upper and lower halves of each mold in order to assist with alignment and ensure the molds are stacked concentric. *Figure 18* shows these pin holes added to the molds.

Figure 18: Alignment pin holes added to the upper and lower halves of the molds

Once the glue was applied on both halves, the assembly was clamped and left to sit for 24 hours to fully cure. After all glue was cured, each mold was sanded using 80G sandpaper until smooth. On the sidewalls of the larger mold, there was an issue where the ShopBot cut small divots into the base portion during machining and these small cuts created pockets when the upper portion was glued on top of them. In order to create a good seal when we layup the carbon and to create a smooth hoop wall, these pockets were filled with Bondo body filler and sanded even with the surrounding MDF. Bondo body filler was also used to fill the holes made when the molds were mounted to the table for the ShopBot using wood screws. When these hoop walls were being sanded, they began to scallop due to the difference in density between the middle

portions of the MDF, the compacted edges of each board, and the glue layers. In order to combat this issue, tools were cut from the scrap circular MDF boards that were remaining from the milling of the upper portions, *Figure 19,* below.

Figure 19: sanding tools made from the inner scrap of the 2D contour

This allowed for a harder, non-deforming surface that would sand down the raised portions, without further scalloping the less dense layers. After a significant time sanding, the hoop walls were checked using a combination square to ensure there was still a 1.5 degree draft angle. In addition to this check, the combination square's edge was also used to verify that the scalloping was no longer present along the hoop walls.

Once each mold was sanded to a smooth, non-scalloped surface, sanding sealer was painted on in three thin layers using foam paint brushes. *Figure 20* shows the application of the sanding sealer.

Figure 20: Application of sanding sealer to the molds, using a foam brush

Each layer was painted on thinly in order to allow for a better dry time and to prevent air pockets and bubbles. The sanding sealer was painted on the top surface and once three full layers were painted and dried, the molds were again sanded, but using 220G sandpaper this time. The purpose of this sanding was to remove the shine from the sanding sealer and to correct any small imperfections before continuing. Once the shine and imperfections were removed a second set of three thin layers of sanding sealer were painted on. After these next layers were fully dry, the molds were sanded, once again, using 220G sandpaper and prepped for polyurethane.

The polyurethane process was similar to the sanding sealer process, however, instead of using paint brushes, the polyurethane was applied with a paint spray gun in order to reduce runs

and inconsistencies in the layers of polyurethane. The set up and process for the polyurethane spray was much more involved than that of the sanding sealer. Due to the colder temperatures and higher wind speeds on the days the molds were being sprayed, a canopy system was set up in order to reduce the possibility of spray errors, seen in *Figure 21.*

Figure 21: Poly spray tent created to protect the spray from wind and weather

A cake decorating, lazy Susan was purchased to make the spraying of the hoop walls easier. Each mold was taken outside under the canopy and placed on the lazy Susan and sprayed evenly with polyurethane. When spraying the polyurethane, it was important to stay the same distance away from the part at all times; it is very easy to want to make a curved path, where in the middle of the path, the gun is held closer to the part. This curved path sprays inconsistent layers on the part and pools the polyurethane in random places. Two layers of polyurethane were sprayed onto each mold and left to cure. The two molds, after the poly spray, can be seen in *Figure 22.*

Figure 22: Both molds curing after polyurethane sprays

Once fully cured, the polyurethane layer was sanded using 220G sandpaper to remove the orange peel appearance and prepped for another spray of polyurethane. After applying and sanding the polyurethane, until adequate coverage was obtained, roughly six layers. The polyurethane layers were polished to a completely smooth finish using 600G and 800G wet sanding paper. A smooth finish was required for the carbon fiber to layup appropriately.

Manufacturing Limitations and Issues

When spraying the polyurethane, the air pressure in the line was very low, despite keeping the spray gun at the optimum setting. This was caused by the air compressor struggling to keep up with the multiple machines running during spray times. Other teams were machining parts on the lathe and Haas mill, which sapped air pressure in the line for the spray gun. This reduced pressure caused a pulsing effect in the spray fan stream, which resulted in a "spitting" of the polyurethane onto each mold. When observing the molds after the spray, blobs and strings of polyurethane were very prominent on the hoops walls and in areas where the overspray was redirected back onto the part. This issue could have arisen due to the cooler temperatures in Colorado when spraying our polyurethane.

Carbon Fiber Layups

In order to prep the molds for the layups, masking tape was placed along the top edges to prevent the mold release from interfering with the application of the bagging tape in these areas, seen below in *Figure 23*.

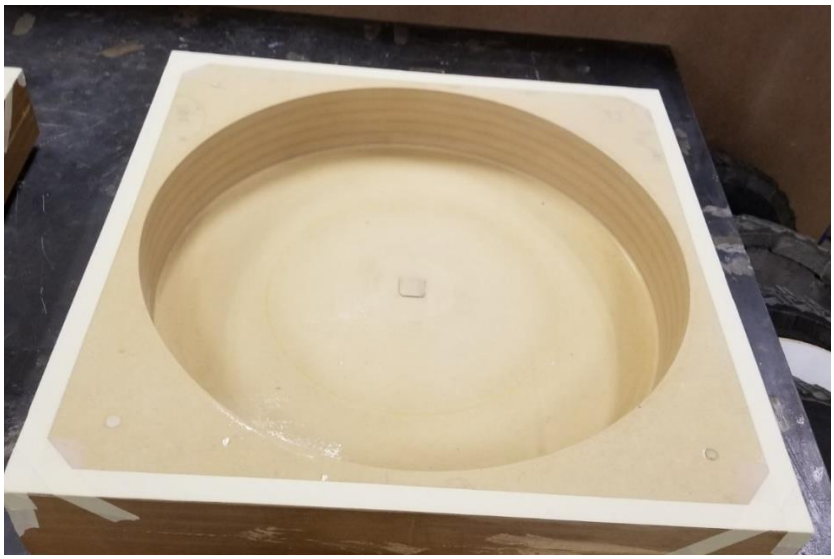

Figure 23: Masking tape added to all upper edges, to prevent mold release from being added there

After ensuring full adhesion of the masking tape on the mold, Zyvax, mold release, was wiped along all faces of the mold. Each layer of Zyvax was fully dried before applying new layers; a total of six layers was added to the mold. Once the mold had all layers of mold release applied, it was then brought into the composites room, which was the “clean room” for more layup prep. Before conducting any layups on the tool, the bagging tape was added, where the masking tape was removed. Pleats were added to the bagging tape to allow for the vacuum bag to fill in the bowl section of the tool. Without pleats, the vacuum bag would be too tight and would not dip down into the lower bowl section of the mold. The pleats were added to the sections of the mold where the wheel’s hoop section was closest to the outer square contour. This allowed the largest portions of bagging to be brought into the bowl section of the mold. The pleats can be seen in *Figure 24.*

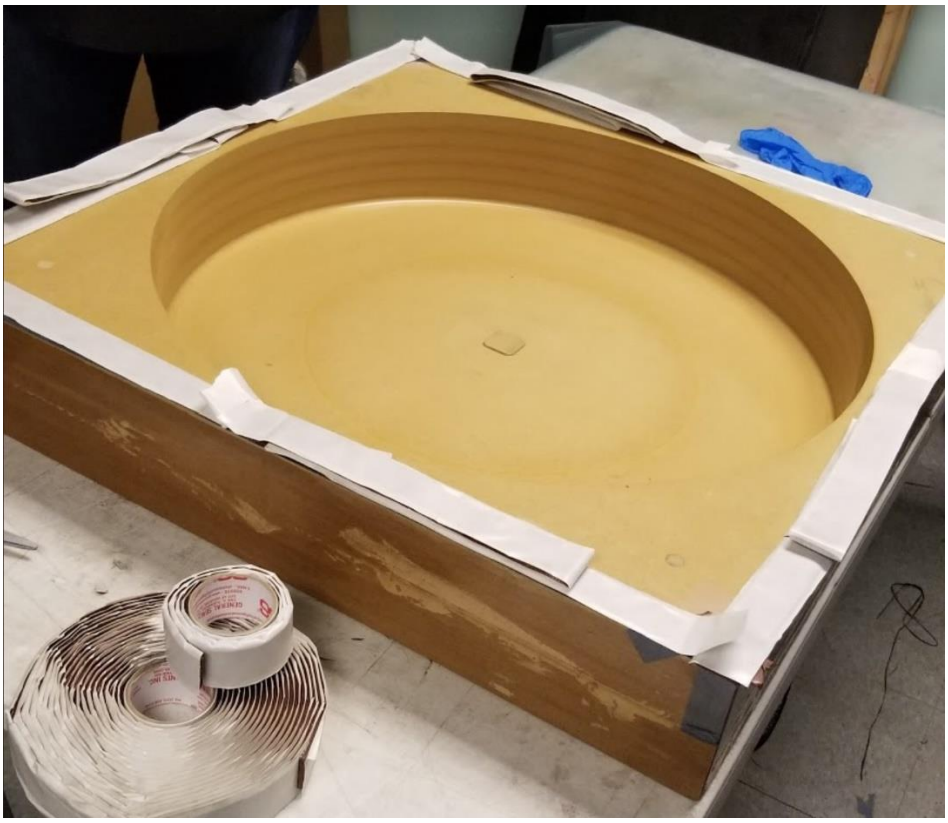

Figure 24: Pleats in the bagging tape

Once the molding tool was prepped for the layup, the carbon needed to be cut and impregnated. The first step in prepping the carbon was cutting bagging material that could sandwich the carbon fabric between to hold in the resin mixture. 76 inches of bagging was cut to accommodate the carbon fiber fabric length required to cut all desired circles and strips. SolidWorks was used to determine the exact length of carbon fiber needed to perform each layup. The diagram for the layups is in *Figure 25*.

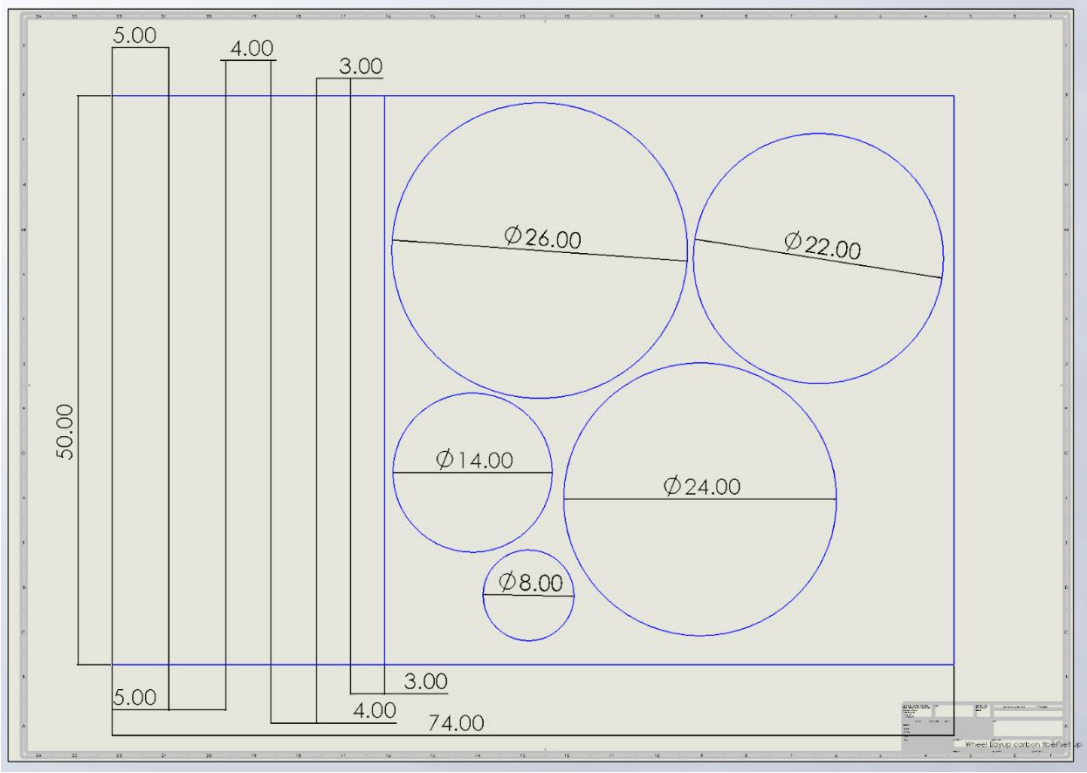

Figure 25: Diagram of the dimensions of carbon fabric needed to accommodate all layers

In *Figure 25* above, there are six rectangular strips in pairs of 3”, 4”, and 5”, in addition to five circles of the following diameters: 8”, 14”, 22”, 24”, and 26”. The five circles had orientations of 0, 45, 90, 45, and 0 degrees, respectively. By diagraming this, it was determined that a maximum length of 74 inches of carbon fabric was necessary to complete one full layup of a shell. The 74 inches of carbon fabric was cut and placed between the two layers of bagging film and the circles and strips were drawn onto the bagging film using a black sharpie, as seen in *Figure 26*.

Figure 26: Sharpie outlines of all needed layers for the layup

Once all the shapes were drawn on the bagging film, the two-part resin was weighed and mixed. The L285 resin required a 40:100 mixture of hardener to resin. Originally, for the first couple layups the resin was weighed to 300g and the hardener was weighed to 120g to keep the correct ratios. After the first three layups, the amounts were increased to 320g and 128g of the resin and hardener, respectively. The reason for the increase in the amounts of resin and hardener used, was to allow for easier spreading to all parts and to reduce the dryness of the impregnated fabric.

The resin was mixed for 2 minutes, until there were no swirls of color and the blue shade was consistent throughout the mixture. The stick used to stir was scraped against the sides of the cup and wiped off on the upper lip of the cup to remove any excess from the stick. After sufficient mixing, the top layer of bagging film was pulled back and the resin was poured directly onto the

fabric, in the locations of the drawn shapes. The top layer of the bagging film was replaced, and plastic spreaders were used to push the resin into the fabric, as seen in *Figure 27*.

Figure 27: Wheels team using plastic spreaders to push the resin into the carbon fabric

The resin was carefully pushed into the fabric at a constant speed and angle; if it was pushed through too quickly, it would not fill the weave correctly with resin and if too much pressure was applied, dry spots would be created. Once the fabric reached a uniform thickness of resin, the shapes were cut and set aside for the layup.

All impregnated carbon fiber fabric portions were brought into the composites room and set aside until needed. Once everything was prepped and ready to go, the carbon fiber was laid up in the bowl section first, starting with the largest diameter circle and continuing to place the circles concentric until the last circle was placed in the mold. When placing the fabric circles into

the mold, one side of the bagging film was removed and the exposed carbon fabric side was centered and placed into the mold, as seen in *Figure 28*.

Figure 28: Placement of the carbon fiber layers into the bowl portion of the mold

Once the fabric was in the correct placement, the top side of the bagging film was slowly removed at a 180-degree angle to prevent from pulling up the placed carbon fabric. As the bagging film was pulled up, paint brushes were used to poke, not brush, the fabric into place and ensure the layer was flat against the mold, as seen in *Figure 29*.

Figure 29: The use of paintbrushes to ensure correct layering into the mold, while the film was removed

After all concentric circles were placed in the molding tool, the varying heights of the hoop side pieces were placed into the mold using the same techniques. To ensure there was no bridging between the carbon and the mold, along the hoop sections, the fabric was placed at the center of each strip first, and was worked into place, moving from the center to the edge. The concentric circle layers and the placement of the hoop fabric can be seen in *Figure 30*.

Figure 30: Concentric placement of circular layers and initial placement of hoop wall layers

When placing the six hoop sections, the upper edge of the mold was matched with the top edge of the fabric section to ensure the hoop section thickness was achieved, as well as, to reduce the amount of carbon trimming required along the upper edges of the mold. Each thickness of hoop fabric was not long enough to span the entire circumference of the hoop, therefore each strip needed to be placed 120 degrees from the previous placement. This ensured that there would be even distribution of all the fabric along the hoop circumference, and prevent any gaps in the layers. Once all circle layers and hoop layers were added successfully to the molding tool, the vacuum bagging prep began. This preparation involved adding release ply, breather cloth, and the vacuum bag, to the mold. When applying the release ply and the breather cloth, strips were pre-cut to, roughly, a 2-inch by 5-inch rectangle. These strips were placed vertically along the hoop walls, while circles of both the release ply and the breather cloth, were

placed on the face of the bowl section of the mold. In addition, multiple layers were added underneath the vacuum puck to prevent the transfer of the patterning of the vacuum puck onto the part. In order to allow the carbon fabric to sit appropriately along the square cut, where the hub will later be installed, an aluminum plate with a similar square cut out was placed onto the mold to provide a better seal with the vacuum along the square. This plate can be seen in *Figure 31*.

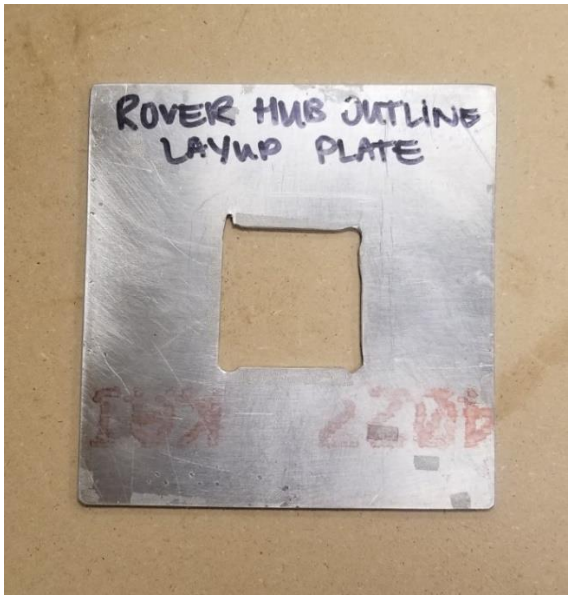

Figure 31: Aluminum plate used to ensure vacuum seal around hub cut out

As soon as all release ply and breather were added to the mold, the bagging process began. The bag was cut in an 80-inch by 60-inch rectangle to ensure all pleats would have enough bagging film material to create the bag.

The bag was applied to the mold using constant pressure and speed along the bagging tape to ensure there were no bubbles or folds in the bagging film material. One side was pressed into the bagging tape at a time. This allowed the bag to be held tight from all angles and made

application much easier. Once all the bagging film was attached to the mold, it was maneuvered in the inner bowl portion to remove any wadding or folding, as much as possible. Then the vacuum line was attached, and the bag was manipulated more, especially in the lower filet area, to make sure it was smooth and not folded at the pleat. Any folds would create bridging in the vacuum bag and would prevent the carbon fabric from taking the shape of the mold correctly. In the case of any bridging in the vacuum bag, a heat gun was carefully used to heat the bagging film, making it more pliable and vacuuming it father into the molding tool. The successfully completed bag under vacuum can be seen in *Figure 32*.

Figure 32: Successful vacuum set up after a layup

The cup used to mix the resin was left with the mold, under the resin was cured inside the cup. This gave the team an indication of when the part was complete and could be removed from the mold. Once the mold was ready to be removed, the vacuum was turned off and the bagging film, breather cloth, and release ply were removed. The part was firmly held into the part after being placed under vacuum for an extended period, ranging from 12-15 hours. Thin plastic tools were used to carefully separate the tool and the part. The removal tools used are seen in *Figure 33*.

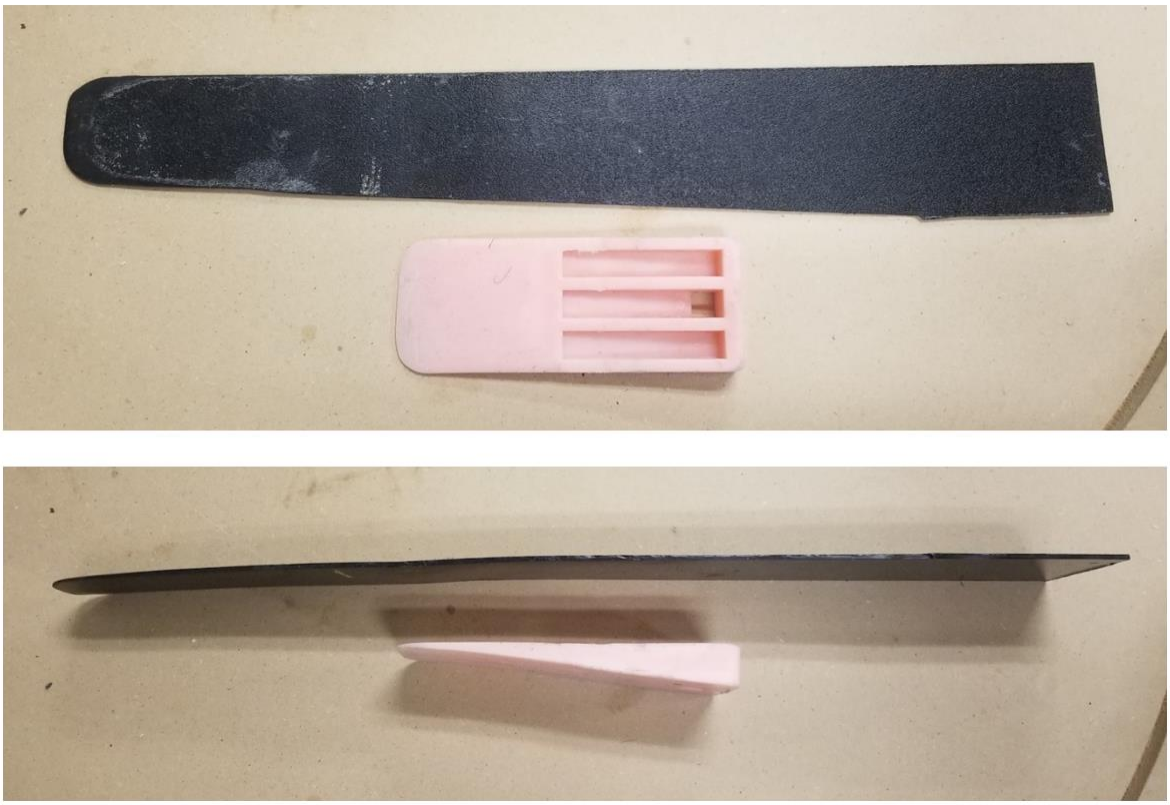

Figure 33: Tools used to remove the cured carbon part from the mold

After the parts were all removed from the molding tools, the edges of the hoop sections and the square cutaway for the hub were cut using an angle grinder. The finished cuts can be seen below in *Figure 34*.

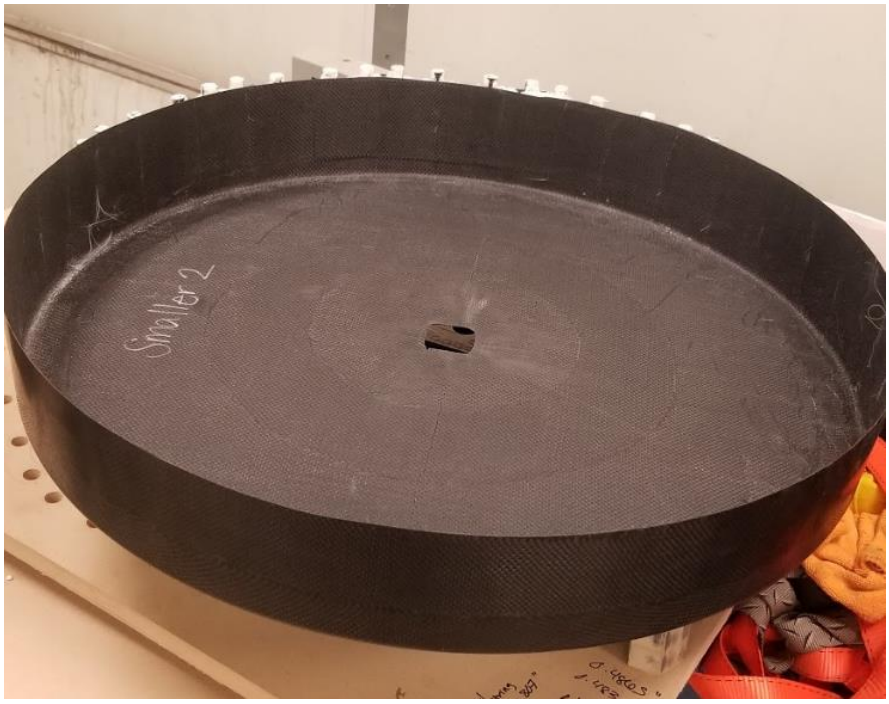

Figure 34: Finished half of carbon wheel shell

Wheel Hub Component Manufacturing

Manufacturing one front wheel hub assembly consisted of manufacturing one hub shaft brake side, one hub shaft bolt side, and three reinforcement discs, per front wheel. Manufacturing a rear wheel required a slightly different set of components, one hub shaft brake side, one hub shaft bolt side, two reinforcement discs, and one rear wheel outer plate. Two front wheels were made in addition to two rear wheels; one spare rear wheel was made. 2-inch

diameter round stock of 6061-T6 Aluminum was used for the hub shaft bolt side and 3-inch diameter round stock of 6061-T6 Aluminum was used to manufacture the hub shaft brake sides and the rear wheel outer plates. 1/8-inch plate of 6061-T6 Aluminum was used to manufacture the reinforcement plates.

Hub Shaft – Bolt Side

Manufacturing a hub shaft bolt side was accomplished using the Haas lathe TL-1, the Trax lathe, the Haas CNC TM-2, and the wire EDM. A finished hub shaft bolt side is seen below in *Figure 35*.

Figure 35: Completed hub shaft - bolt side

The Hass lathe made horizontal passes to cut away the material. Since right and left faces were on the part, both left- and right-handed lathe tools were needed. With the left-handed lathe tool, the far edge was faced, then a finish facing pass was made. Then the left-handed tool made roughing passes on the part to cut most of the interior wide groove away before making

the finishing pass. The tool was changed to the right-handed tool and the other side of the groove was cut. Standard sizes for the cutting tools were assumed, which was a mistake. The left-hand tool was a different standard size, so the part was cut incorrectly, and the results are seen in *Figure 36.*

Figure 36: Incorrect cut on a hub shaft piece

The CAM program thought the tool was a different size, therefore the backside of the lathe tool cut into the hub shaft on the right-hand side as seen in. This unintentional cutting resulted in the right-hand side of the hub shaft being smaller in diameter than designed. After checking the tool sizes and adjusting the tool definition in Fusion 360 to match the lathe tool, the turnings were completed successfully. Refinements in the machine offsets were used to correct cosmetic details of shaft diameters where the two lathe tools cut diameters were different by a couple thousandths. Four acceptable parts were turned on the Haas Lathe. There was debate on how to drill the hole, ultimately instead of milling the hole on the Haas TM-2, The parts were placed into the four-jaw chuck on the Trax lathe and drilled using the tailstock. Next, soft jaws were made to clamp the part in the TM-2 Haas and the square was cut out from the stock on the

left side. Lastly, the part was put in the wire EDM. The wire was threaded through the hole in the part and then through the rest of the machine and cutout was created for the keyed axle as seen in *Figure 37*, below.

Figure 37: Keyed axle-way cut into the hub shaft - bolt side

Hub Shaft – Brake Side

The hub shaft brake side is part of every wheel, so four were made. A complete part can be seen in *Figure 38*, below. The part was machined from 3-inch round bar stock of 6061-T6 Aluminum.

Figure 38: Completed hub shaft - brake side

The four Hub shaft brake side parts were manufactured using the TL-1 Haas lathe, the TM-2 Haas CNCl, the power tap, and the Wire EDM machine. First the 3-inch round stock was chucked in the lathe, the material was faced, and the basic profile was created. Then, the lathe used a groove operation and a round groove cutter to cut the groove and fillet in the part. Then a ¼-inch hole was drilled down the center of the part using the tailstock a center drill and a ¼-inch drill. Lastly, it was parted on the lathe using a parting tool. Soft jaws were used to clamp the part in a vice on the Haas CNC and the six holes were drilled using a 4.2mm drill. When the part was turned over, the square profile seen in *Figure 39,* below, was milled, and the glue relief lines were engraved.

Figure 39: Square milled portion and engraved resin relief lines

The six holes were deburred then tapped using an M5x0.8; the power tap was used for speed and quality. Lastly, the wire EDM was used to cut the shaft hole. A wood dowel was used to push spent wire buildup down the exit shoot to the waste receptacle. *Figure 40*, below, shows a typical wire buildup that causes the machine to stop until the wire is cleared and the machine is commanded to start up again.

Figure 40: Wire EDM buildup near the exit of the machine

After many wire clearings the EDM finished machining the shaft-keyway hole. A finished cut is seen in *Figure 41*, below.

Figure 41: Finished axle shaft cut after the wire EDM

Figure 42 shows the mounting that was used for the part on the wire EDM. During the machining of the keyway, a sliver of the mounting plate was cut loose and created a point of contact that created an error in the machine while cutting.

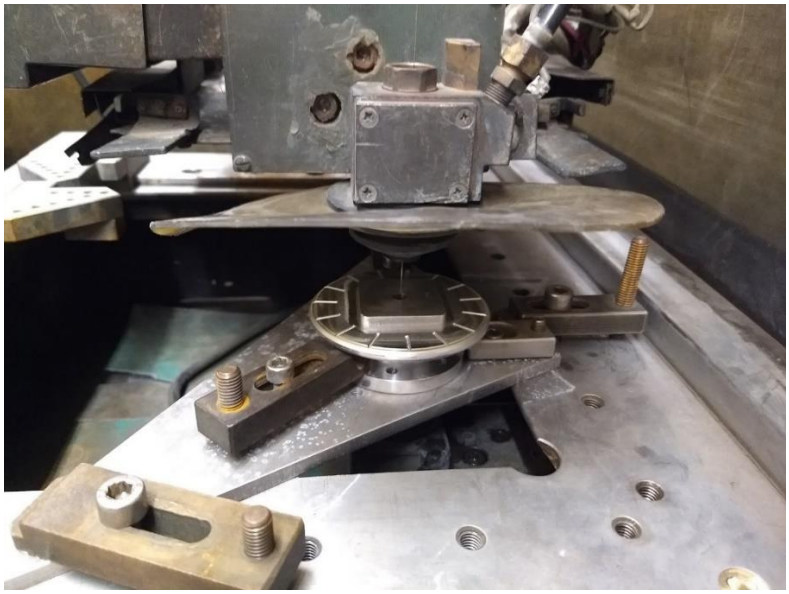

Figure 42: Set up in the wire EDM to cut the keyed axle shaft

Reinforcement Plate

Each wheel has multiple carbon fiber reinforcing plates that help affix the carbon fiber to the hub shaft. The front wheels use three plates and the rear wheel uses two plates. Ten plates were needed to accommodate two front wheels and two rear wheels. The plates were made, three at a time, in the Haas TM-2 CNC via patterning. Due to the patterning constraint, 12 plates were fabricated as shown in *Figure 43,* below.

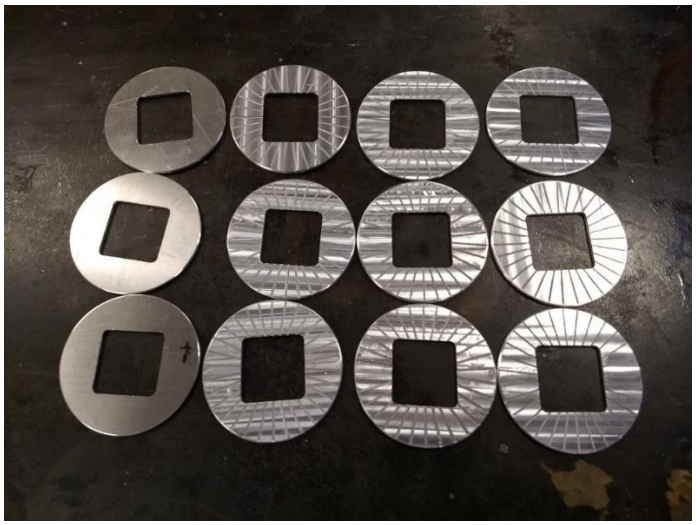

Figure 43: 12 reinforcement plates machined

The plates were machined to a thickness of 0.100 inch from 1/8-inch plate stock. Then, the square hole was milled, and the radial grooves were engraved. Next, the clamping needed to be adjusted so the parts would not fly free when the exterior circle was cut, so machining was paused, the middle of the part was cleared, and each plate was clamped down through the middle. Then the exterior circle profile was cut. To create a set of three plates, the stock material was cut into appropriately sized rectangles. Rounding the exterior circle of the plate was accomplished by manually creating a jig to hold a single plate on the lathe, and then manually adding a chamfer on both sides of the part, which was then rounded. The setup for this is seen in *Figure 44*, below.

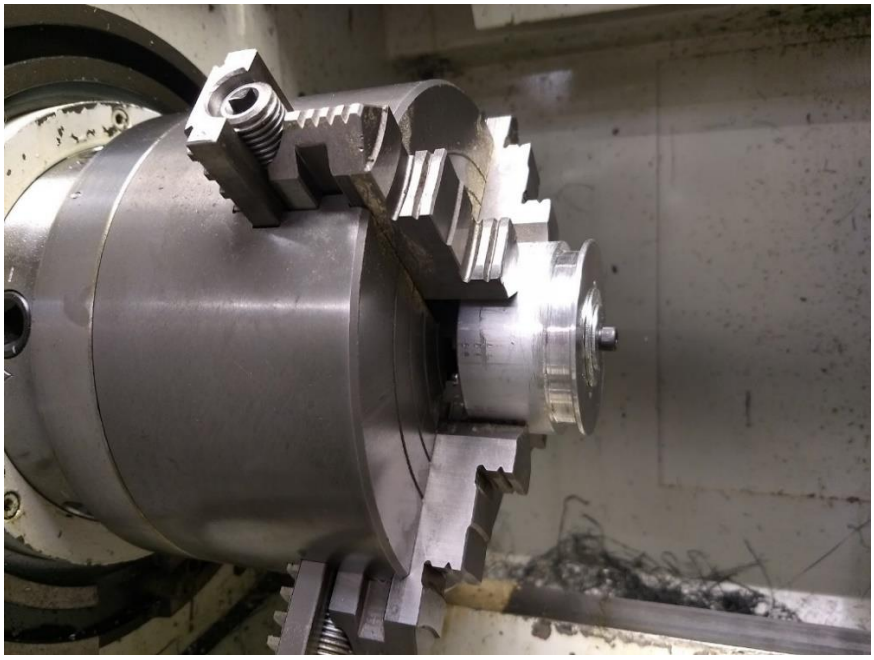

Figure 44: Set up required to cut chamfers and fillets into the edge of each reinforcement plate

Rear Plate

The last component of the wheel hub is the rear plate. This component is only used on the rear wheel, so only two were manufactured. Similar to the hub shaft brake side, this part was machined from 3-inch round bar stock of 6061-T6 Aluminum. The profile was turned down on the Haas Lathe and then the faces were machined on the CNC.

Figure 45: Rear plate prior to the cutting of the axle keyway

Figure 45, above, shows one side of the rear plate before the keyway was cut. At first, a plunge cut was attempted on the lathe, but there was tool deflection that occurred when cutting the shoulder on the plate. This resulted in the shoulder of the part being at an angle instead of flat with the bottom. The cut was changed to a horizontal pass tool cut and the exterior profile was successfully cut. Then the center hole was made on the lathe using the tailstock and a ½-inch drill. The rear plate was parted off from the stock and a second part was made.

Next, the round blank was secured in the Haas TM-2, using soft jaws in the vice, and the six holes were drilled with a 4.2mm drill. The part was flipped over, and the bottom was machine flat. A square profile was cut into the part and radial lines were engraved. These operations can be seen in *Figure 46*.

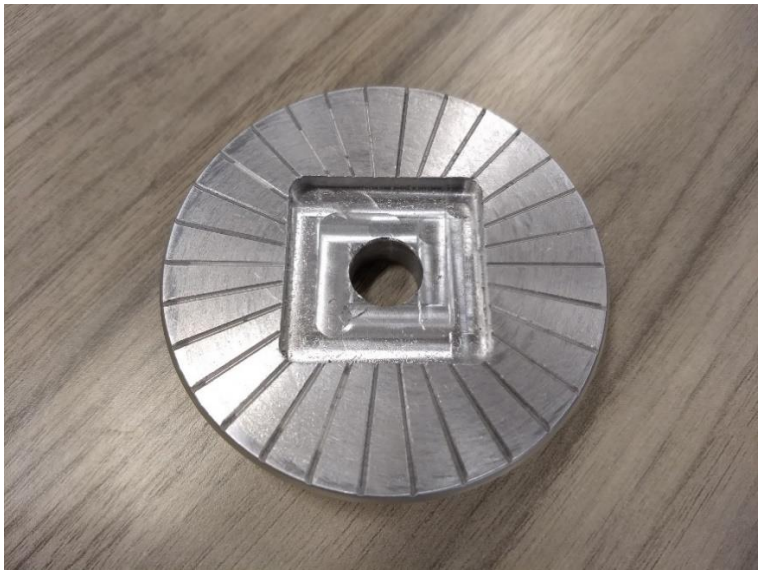

Figure 46: Square profile cut and radial resin relief lines included

Once the CNC operations were complete, the holes were tapped using the power tap with an M5x0.8 thread. Lastly, the hole for the keyed shaft was cut on the EDM wire, like the hub shaft bolt side and brake side parts. Since the rear plate is considerably thinner than the shaft parts it was cut significantly faster on the wire EDM.

Moving Forward

Once all the wheel hub components were completed, the wheels would be assembled. The reinforcement plates will be affixed to the carbon fiber wheel shells. 10-oz fiberglass will be used as a scrim between the reinforcement plates and the carbon fiber wheel shells to prevent the clamping pressure from squeezing all the adhesive out. Between the carbon fiber wheel shells, the same resin that was used for the carbon fiber layups will be used, however, micro-balloons will be added to increase viscosity of the resin so it does not leak out. To keep everything

concentric all the wheel hub and carbon fiber components will be assembled at one time and the keyed 17mm axle will align the shells and the hub parts concentrically. Separately, the rubber tread will be poured into a mold made of MDF with an inner groove for a shell of bendable wood board to be the inner ring of the rubber for the mold. An outer groove will be created to slot pegs from the 3D printed tread pattern.

Endeavour Suspension

Previous Design Constraints

In 2017, two pairs of A-arms were created to connect the frame to the front two wheels, allowing the front system to compress and expand with the shock supports. Each shock is connected to the lower A-arm, at the cross-sectional bar, as seen in *Figure 47*. The A-arms have a considerable range of motion that allows for the frame to smoothly move up and down in the y-axis as the wheels navigate the rocky terrain of the course. However, when these A-arms were designed, the connecting tie rods, that attach the A-arms to the knuckle, were designed with single shear mountings.

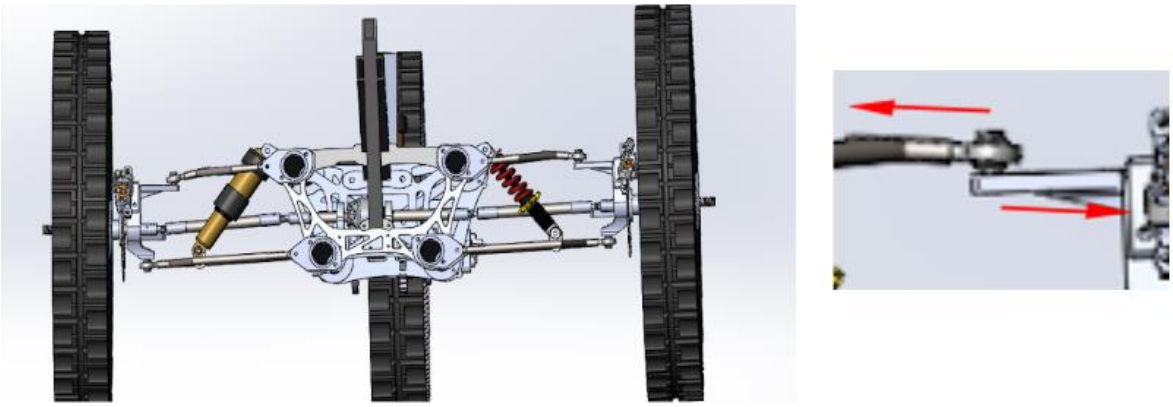

Figure 47: Previous suspension connection system in single shear

Although the system was still allowed to function properly with single shear connections, it was decided that a redesign of double shear connections would be appropriate for increased stability and less chance of failure during competition. The force of the tires opposing the connection at the end of the A-arm point is split in two, and evenly distributed on either side of the tie rod while the tie rod's reaction force acts in between.

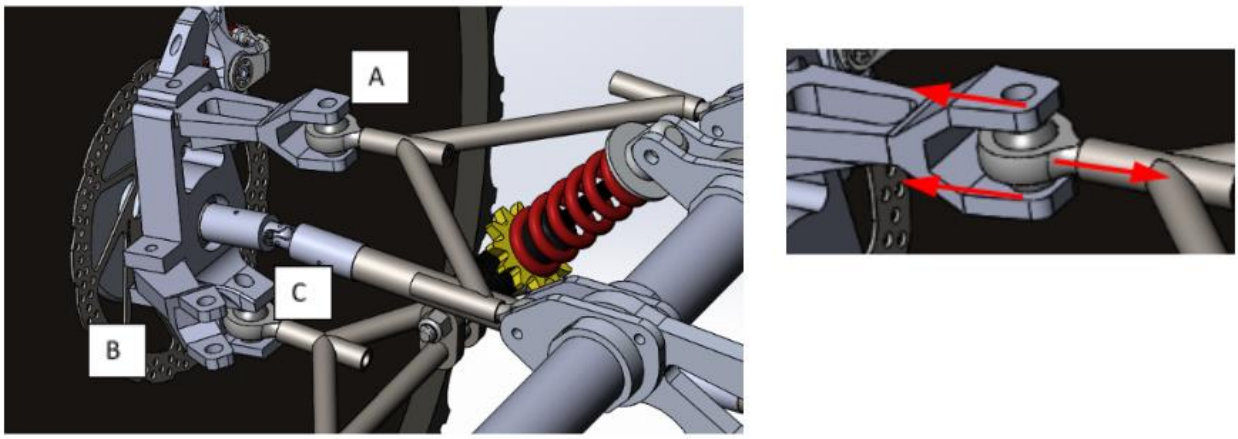

Figure 48: New suspension design with double shear

Modified Design of Double Shear Connections

Double shear connection points were made on either side of the front frame suspension for both sets of A-arms and for the tie rods that would be connecting the wheels to the modified steering system. In *Figure 48*, parts *A* and *B* are separate from the knuckle piece that connects the wheel to the system and are bolted in place, while part *C* was a modified extension to a pre-existing connection on the knuckle. Each piece that was made into a double shear connection maintained the original thickness of the previous parts, in order to fit properly within the knuckle. It was discussed that the knuckle, and the connecting pieces, could potentially be made using thinner thicknesses to reduce the weight of the entire system. However, due to the time constraint of this project, and given that the existing design satisfies the approximated force analysis, it was unnecessary to change these parts.

Endeavour Steering

Previous Design Constraints

The steering mechanism designed by the previous team included an Ackermann Pitman arm under the seat of the front driver that connected to a linear rod and bearing system. The linear rods were attached to the driver's left and right side and moved in and out of linear bearings. At the end of these linear rods, tie rods connected to ball joint ends that then connected back to the Pitman arm. However, as the Pitman arm would move, the linear arms did not account for the height adjustment of the tie rods.

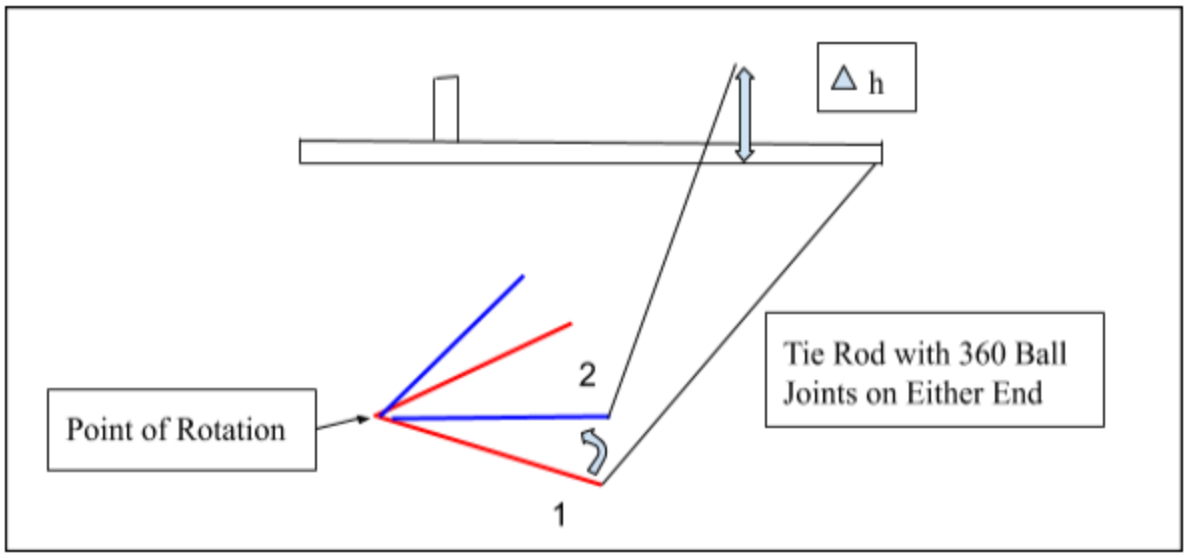

Figure 49: 2018-2019 Red Rover Steering

As demonstrated in *Figure 49*, the Pitman arm moves from point *1* to *2*, and the tie rod is not allowed to adjust for the height difference, *Δh*, because it is bound to the connection point of the linear rod. It was also noted that as the vehicle would navigate the course, torsion in the frame caused the linear rods to misalign and jam within the linear bearings. When the linear rods misaligned, it would restrict the driver from continuing the linear motion of the handles connected to the rods and therefore disable the steering system.

Current Steering System Design

In order to turn the wheels, a tie rod is attached to the knuckle of each wheel using a supers-swivel ball joint that is fastened to an attachment in double shear. Each tie rod attachment that is bolted to the knuckle, will be fashioned in a way such that the tie rod

attachment point will be in line with the wheel rotation point and the center of the back wheel. This will allow the system to have 100% Ackermann Geometry.

The opposite end of each tie rod is connected to a small radius pitman arm located underneath the driver's seat, and pivots on a shoulder bolt about a double shear hinge attached to the lower half of a bulkhead. The pitman arm rotates proportionately to a larger radius that is pushed by the handles, and greater stability is attained for the whole steering system, by adding a second identical pitman arm with the same larger rotational geometry. It is offset it from the bulkhead with a large square 5-inch bracket so that a parallelogram is made by adding hollow square connecting rods, giving an approximate straight line of motion in the handles. These pivot points are also supported by steel shoulder bolts.

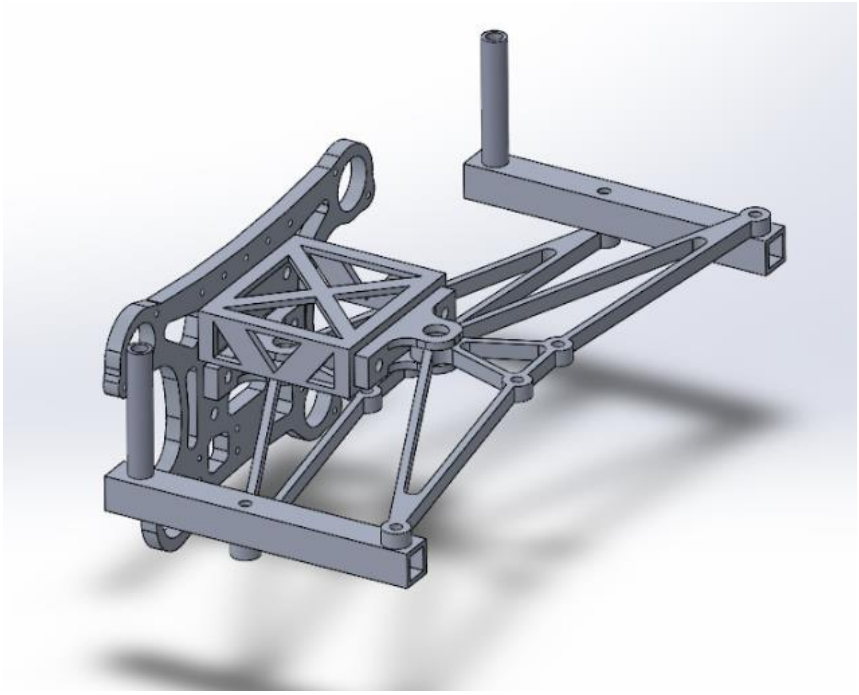

Figure 50: Current Steering System Design

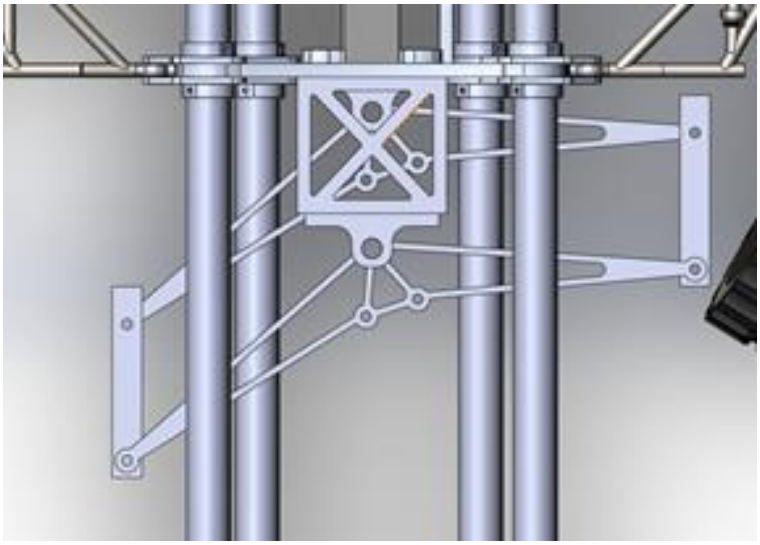

Figure 51: Top Down View of Current Steering System

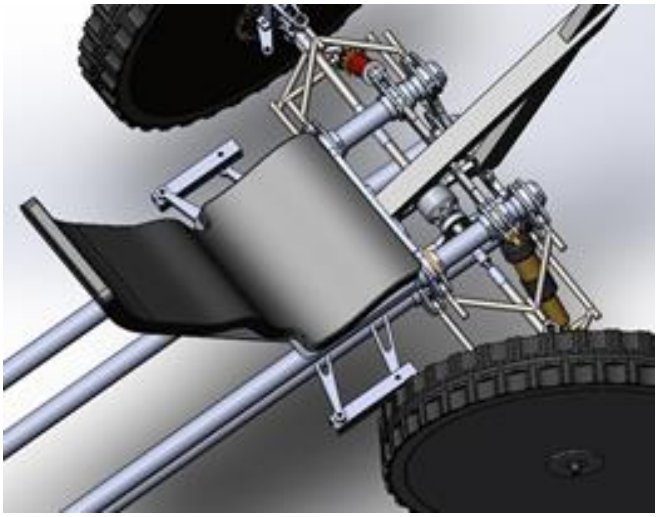

Figure 52: Top Down View of Current Steering System on Rover Assembly

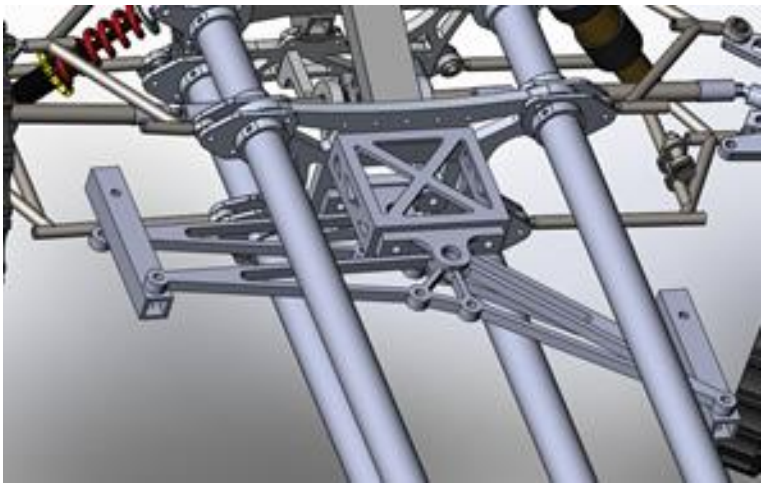

Figure 53: Close-up view of bracket extending second pitman arm

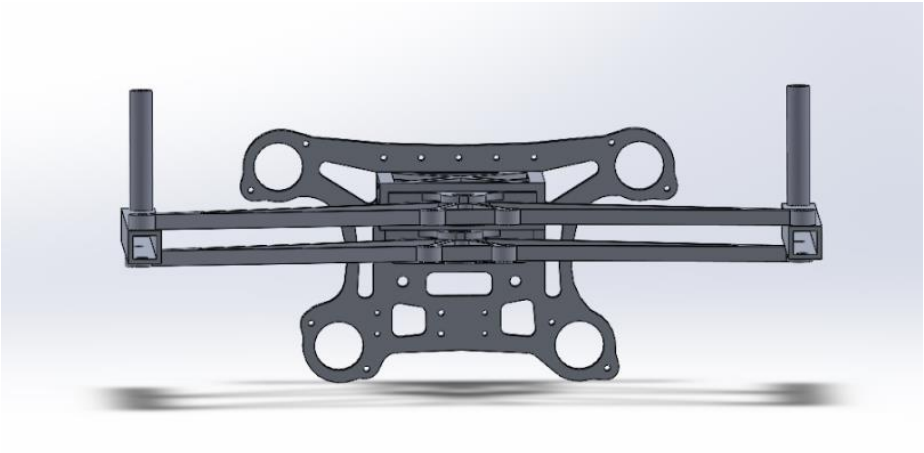

Figure 54: Rear View of Current Steering System

The longer ends of the additional pitman arm are fastened to the top of each square bar using shoulder bolts five inches past the placement of the first pitman arm on the underside.

A handle made from a hollow aluminum 6061-T6 rod will be welded to the opposing ends of the square bars and will be placed on the right and left sides of the driver in order to steer the vehicle. When the driver pushes the left handle forward, and pulls the right handle backward, the approximate linear motion obtained from the parallelogram is transmitted into the small angular motion of the tie rods by rotating both pitman arms in a clockwise fashion. The rotation

of the lower pitman arm creates a smaller turning angle for the left, outside tire and a larger turning angle with the right, inside tire; this motion ultimately turns the vehicle to the right. If the driver operates the vehicle by pulling the left handle back and pushing the right handle forward, the pitman arm mirrors the right turn, turning left with a larger turning angle for the left, inside wheel and a smaller angle for the outside wheel, following Ackermann steering geometry.

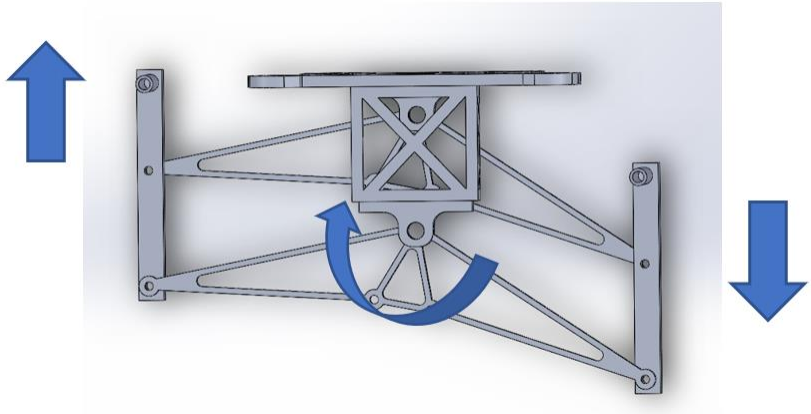

Figure 55: Top Down View of Steering System turning Vehicle to the Right

When the handles are thrusted forward and pulled backward to control the direction of the rover, the square bars will move slightly in towards the vehicle when executing a turn, and slightly away from the vehicle when pulling out of a turn. The Denver Endeavour has been working with Don O'Connor, owner of Any and All Bikes. Don has assembled and sold recumbent bikes to professional athletes for over twenty years. For the rider to not overexert unnecessary strength, Don has recommended that the handles be placed the same distance apart as the width of the driver's shoulders. Due to the constant motion of the handles linearly pulling into and away from the driver, the shoulder width of the driver was considered as the neutral width of the handles for when the vehicle is not turning. However, due to the constraints of the seat and

distance between the upper stringers, the ultimate neutral width of the handles is 22 inches, which is more than the driver's shoulder width. This can be fixed by adding bends in the handle to bring it above the stringers and inward to be parallel to the driver's shoulder width.

Ackermann Geometry

Initially, it was decided that an Ackermann steering geometry, combined with two Peaucellier linkage systems would be utilized to transform exact linear motion control from each handle to small angular motion to turn both wheels. However, the Peaucellier linkage system was too complex and it was questionable whether it would be capable of withstanding the forces required to turn the wheels, which allowed for many possible points of failure. A simpler system was designed to continue utilizing Ackermann geometry, but only approximating a straight line of motion for the handles, rather than the exact straight line obtained with Peaucellier linkages. We continue to use Ackermann geometry due to its consideration of the angle of rotation of each wheel to minimize slipping.

"Ackermann steering mechanism, *RSAB* is a four-bar chain as shown in fig.1.50, [within *Figure 56]*. Links *RA* and *SB* which are equal in length are integral with the stub axles. These links are connected to each other through track rod *AB*. When the vehicle is in straight ahead position, links *RA* and *SB* make equal angles α with the centerline of the vehicle. The dotted lines in fig.1.50 within *Figure 56* indicate the position of the mechanism when the vehicle is turning left." (Tutorials, 2013)

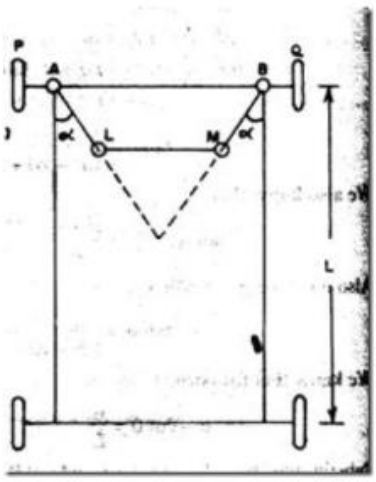

Fig.1.49: Ackermann steering gear mechanism

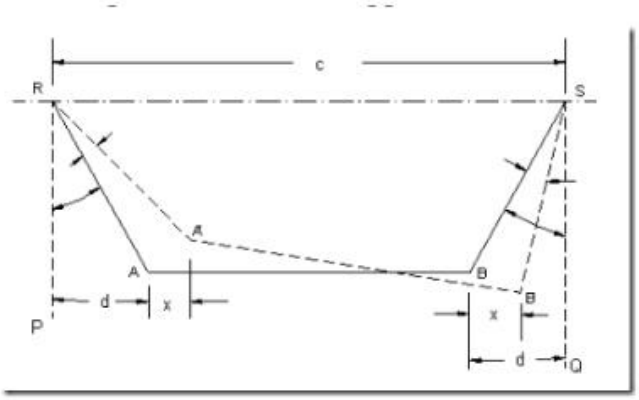

fig.1.50: Ackermann steering gear mechanism

Figure 56: Steering Mechanisms: Kinematic of Machines, Ackermann Steering Geometry (Tutorials, 2013)

The figures above illustrate Ackermann geometry and demonstrate the theory behind the Ackermann linkage used in the modified steering system for the Endeavour. The Ackermann linkage is represented by the segment *AB*. Segments *RA* and *SB* are equal in length and are represented by the tie rods connecting the rotational motion of each pitman arm the tie rod attachment connected to the knuckles on the left and right wheels. When the track rod is horizontal, as seen as segment *AB* in fig.1.50 from *Engineering Tutorials*, the angles between the connecting segments and the length of the system are equal. As the system turns to the right, or the left, the angle is increased on the inner side and decreased on the outer. This provides a tighter angle of rotation from one of the tires and a larger angle of rotation from the other tire, allowing both to remain parallel in direction.

The maximum turning angles necessary for the vehicle to make due to a minimum 15 ft turn radius required by the competition guidelines were calculated using the following formulas:

$$\delta_o = tan^{-1}\frac{L}{\left(R + \frac{t}{2}\right)} \quad (3)$$

$$\delta_i = tan^{-1}\frac{L}{\left(R - \frac{t}{2}\right)} \quad (4)$$

Where δ_o represents the outside turning angle, δ_i represents the inside turning angle, *L* is the vertical length of the vehicle from the center of the front tires to the center of the back tire, *R* is the turn radius, and *t* is the horizontal width of the front tires from center to center (J.Y. Wong.) The calculations for the Endeavour are shown on a spreadsheet in *Appendix B.*

Calculations of Forces Applied to Wheels

In order to ensure that the steering system has a safety factor of 2, the force applied perpendicular to the wheel on the tie rod attachment was determined by the following equation

$$F = \left(\frac{a}{l_k}\right) \times F_y \quad (5)$$

The variable l_k in *Equation 5*, is a representation of the linear distance in the x-direction from the center of the front wheel to the tie rod attachment where the tie rod end is placed, F_y is the thrusting force within the tie rods, and *a* is the trail of the tire.

$$a = \varphi R \quad (6)$$

The trail of the tire *a*, in inches, is the product of the caster angle, φ in radians, and the tire radius *R,* in inches. The caster angle is defined in the text, "…the steer rotation axis is inclined in the longitudinal plane. Positive caster places the ground intercept of the steer axis ahead of

the center of tire contact" (Gillespie). The caster angle is the angle between the vertical axis of the centroid of the tire and the inclination of Kingpin axis along the knuckle.

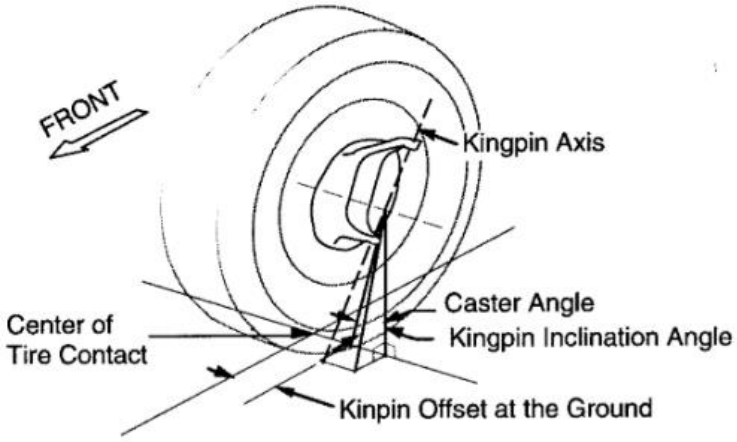

Figure 57: Caster Angle created between the center contact between the ground and the tire with the inclination of the Kingpin Axis. (Fig 8.8 Steer Rotation Geometry at the Road Wheel (Gillespie))

Finally, to complete linear thrusting force *Equation 5*, the force acting perpendicular to the hubs of the front tires was determined by equation $F_{y,f}$.

$$F_{y,f} = \frac{l_R}{L} m \left(\frac{V^2}{R}\right) \tag{7}$$

Where l_R is the length in the x-direction, from the center of gravity of the vehicle to the center of the rear wheel, in inches, L is the distance between the center of the front tires to the center of the back tire in inches, m is the mass in lbm, V is the average forward velocity of the vehicle in feet per second, and R is the tire radius in feet.

The required force F applied perpendicular to the wheel to steer the vehicle was calculated to be 120.44 lbf. The average angle between the tie rod and the axis perpendicular to

the face of the wheel is about 15 degrees, making the force necessary for the tie rod attachment to push at that angle to be 125.56 lbf. The tie rod is connected to the smaller 2.5 in radius of the pitman arm and it must overcome this force. The longer arms pivoting on the same pitman arm gives a mechanical advantage for pushing and pulling the handles proportionate to the larger 11.9 in radius, resulting in a necessary thrusting force of 26.28 lbf. According to Canadian Centre for Occupational Health and Safety, a person seated has an average pulling and pushing force of 29 lbf (Safety). The Occupational Safety and Health Administration of the United States Department of Labor limits this to a maximum pushing force of 50 lbf (Occupational). This implies that the force required to steer the rover is well within these limits, and the driver of the vehicle should be able to exert this amount of force naturally. Free-body diagrams of these forces can be seen in *Figure 58*.

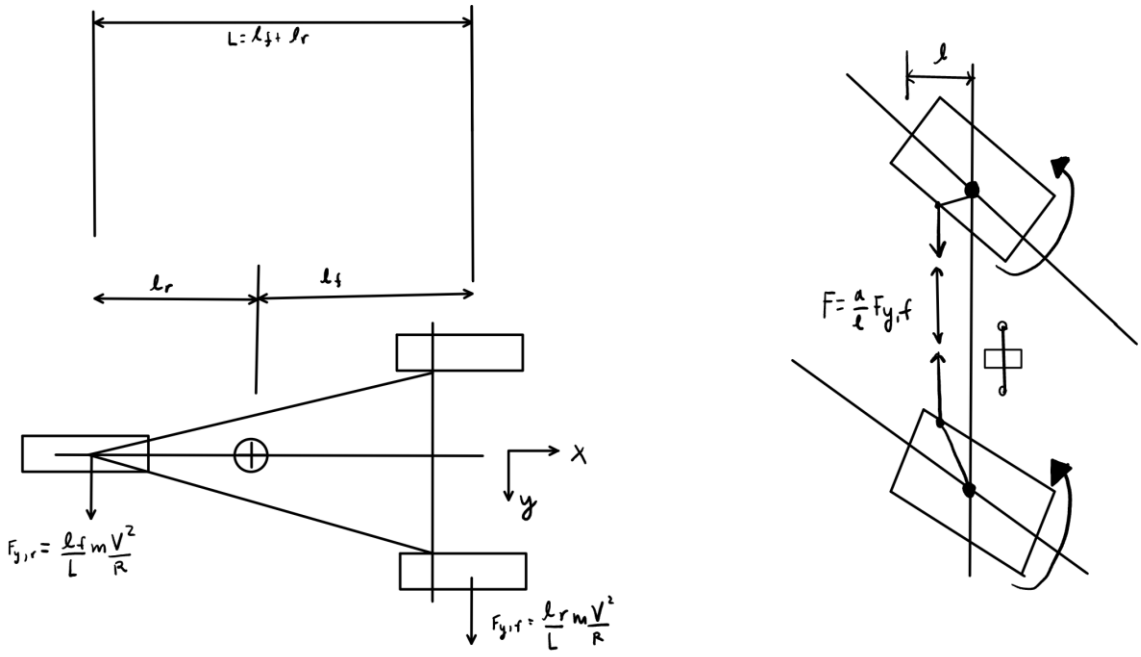

Figure 58: Free-body diagrams of steering design

Assistance in determining these equations and diagrams, was given by Professor Joseph Cullen of the Mechanical Engineering Department at the University of Colorado, Denver. The calculations for the Endeavour rover can be seen in *Appendix C*. Motion analysis between the tie rod attachment and the inner pitman arm must also be carried out in order to ensure the full steering motion is able to be made.

Limitation and Analysis

The new steering system is attached directly to the bulkhead with double shear brackets and is not supported by any structures on the frame. In order to add stability to the system and minimize bending the pitman in the vertical direction, a parallelogram is made to keep the system in a flat horizontal plane, pivoting around vertical shoulder bolts bracketed to the bulkhead. The only forces being applied to the system, other than its own weight pulling it down, is from the tie rods onto the connection points on the pitman arm. This force is constantly changing its effects on the pitman arm because of the changing angle throughout the turning motion. The motion of the tie rod attachment and the pitman arm have not been finalized due to previous spatial constraints with the suspension and because the steering system design was altered completely after the midterm. The thrusting force required to maneuver the steering system was found to be F = 124.5 lbf. The force applied to the steering system during finite element analysis was doubled to F = 249 lbf in order to ensure a safety factor of at least 2. FEA was attempted on some of the smaller and manageable parts like the handle and connecting rod, but SolidWorks had a difficult time not crashing when analysis was attempted. When the final

motion and dimensions of the pitman arm and tie rod attachments are made, FEA will likely need to be done by hand in order to prove each part has a safety factor greater than 2.

Bulkheads

Two bulkheads were designed in order to provide placement for the new steering mechanism of the Denver Endeavour rover. The first bulkhead was designed to replace last year's bulkhead, providing the placement of new collars supporting the A-arms for suspension. This redesigned bulkhead must provide stability to the entire frame of the rover and is especially crucial because it is placed directly behind the driver's seat. This bulkhead will also support the front differential and bolt the front of the frame that supports the pedals and gearbox, as teams have done previously. Much like the Red Rover team, a pitman arm is placed on the bulkhead using bushings and bearings to allow for the most efficient rotation. However, the orientation of the holes to place the pitman arm will be different than Red Rover, so a new bulkhead must be manufactured out of the same 6061-T6 Aluminum. Contours were cut out of the body of the bulkhead in order to lessen the material weight, while still maintaining a safety factor above 2 while including the correct placement of holes being used for supporting other parts of the rover.

The new steering system utilizes a parallelogram-like dynamic motion, so a second, brand new, bulkhead must be manufactured to support the second pitman arm that is placed 6 inches behind the first one. This bulkhead will not provide any support for anything on the frame, other than reducing torsion of the rover, by supporting the rigid placement of the carbon fiber stringers. The new parallelogram steering design necessitates a second pitman arm to be

connected to the first by a bar on either side, and holes for the placement of the bearings supporting that pitman arm will be an inch above the first one because the bars connecting the pitman arms will be a square inch on the outside. Contours are also placed on the sides of the bulkhead to reduce stiffness and allow for the front pitman to rotate fully when moving the handles for steering. This bulkhead is also made of 6061-T6 Aluminum.

Handles

The handles will be connected to the bar between the pitman arms but will be made of steel rather than aluminum to reduce bending. The steel handles will be wrapped in a foam tape in order to provide more grip when steering the rover while minimizing the weight added. The connecting bar between the pitman arms will be a hollow aluminum square bar, 1 inch on the outside and 0.125” thick. It is crucial for these bars to remain stiff and not bend due to the forces being applied to them because that would cause the parallelogram system to fail and prevent full steering motion. It is also important for the handle, itself, not to bend so all the driver’s energy is being transmitted directly to the motion rather than resisting the bending of the metal.

Pitman Arms

The pitman arms were made using Aluminum 6061 material and were manufactured using a CNC machine. Once a safety factor of 2 was verified through FEA using Fusion 360 CAD modeling, the set up for the CNC machine was made using the program’s CAM feature. The counterbores for pressed fit bushings, top counter sinks, and cut outs that were designed to

reduce the part's overall weight, were cut first in order to hold the stock material in place within the vice. Then the outer profile was cut using a ½" flat end mill. After the top side was manufactured, the part was turned over to the other side and clamped within the machine in order to create the counter sinks for the oil embedded bearings. Considering that the part could not fit symmetrically within the soft jaw vice of the CNC machine, an alternative was created in order to create the counter sinks on the other side of the part. Each counter sink was created separately, and the datum was reset each time to be the center of the previously cut bore holes in order for the counter sinks to be concentric.

Once the pitman arm was completely manufactured on both sides, bronze bushings were press fit into the ends and center points of rotation for the pitman arms. This was done by heating the aluminum with a blow torch to expand the bore hole prior to pressing the bushings in using an industrial press. In order to create a snug fit, counterbores were created to be 0.001 inches smaller per inch of diameter of the pressed fit bushing. In order to be more cost effective, steel bushings were created out of steel tubing for the steel shoulder bolts connecting the pitman arms to the moving tie rods. Steel bushings were precisely cut from a rod using a lathe, as seen in *Figure 59*.

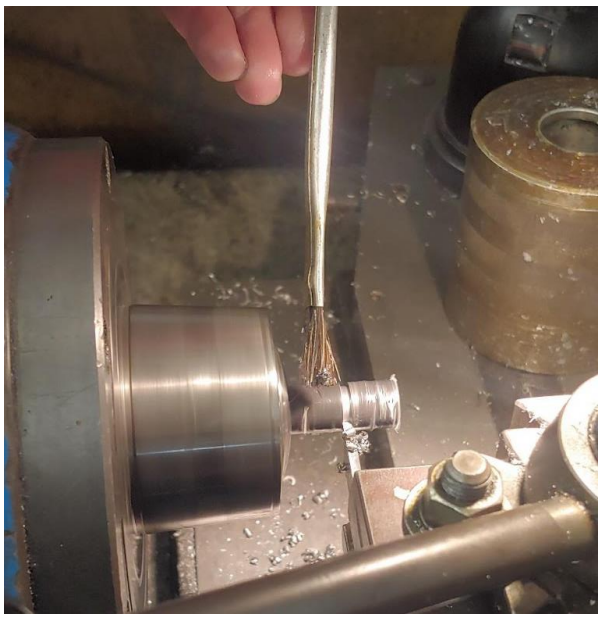

Figure 59: Bushing being cut on a lathe and oil being applied during cutting to prevent heat transfer

Material was then pushed up into a diamond pattern, by knurling, to increase the outer diameter and create a proper pressed fit between the bushing and the aluminum, as seen in *Figure 60.*

Figure 60: Completed and knurled steel bushing for the pitman arms

It is important to insert a bushing between a steel shoulder bolt and an aluminum piece so that the steel does not wear an elliptical pattern within the aluminum. Due to its lower Brinell hardness value, aluminum will deform easily over time with the constant wearing of the hard steel around the bores. This will eventually create an elliptical pattern within the aluminum bore. Bushings in between the steel and aluminum act as barriers against this in order to keep parts concentric and rotation symmetric.

The bronze bushings and bearings that were used are oil-embedded and contain heavy duty grease between them and the steel shoulder bolt to reduce friction between parts. This creates a smooth transition of motion when controlling the steering system. Bronze bearings were inserted on the top and bottom of bushings for the center points of rotation and the pitman arm ends. These bearings resemble thick washers and were placed in the counter sinks of the pitman arms using a 0.0005” clearance fit. The bearings will contact the opposite rotating part and decrease friction between it and the pitman arm. It was recommended to use shrink fitted washers on the top and the bottom of shoulder bolts in order to trap heavy duty grease within the bores. However, due to the low speeds of the vehicle it is unlikely that the enough grease will escape and will have to be replaced before competition. If the vehicle was not man powered, but electric and therefore could travel at much higher speeds, shrink fitted washers would be appropriate considering that grease would quickly escape the bearings and bushings.

Collars

The collars were remade in order to account for the change in caster angle of the uprights. The new caster angle shifted the top A-Arm towards the back of the vehicle while shifting the bottom A-Arm towards the front of the vehicle. This created a 3.38° caster angle between the A-Arm connection points and the center of the tire. Since the bulkhead placement on the stringers was fixed, the collars were adjusted to overcome the shifting of the A-Arms. This was done by increasing or decreasing the thickness of the collars connecting the A-Arm using a step design, as seen in *Figure 61.*

Figure 61: New collars for the bulkhead. On left, a step-down tab; on right, a step-up tab

Uprights

The uprights were created using Aluminum 7075 due to its higher strength and similar light weight to Aluminum 6061. The top and bottom connections for the A-Arms were formed into double shear connections and the break attachment was joined to the upright making a

single, cohesive piece. The top attachment was made separately from the upright and is inserted into a square cut out within the upright. The two pieces are then bolted together from the top of the upright. Originally, the top attachment was designed as one piece with the upright, but the overall depth of the entire knuckle would have been close to 4 inches. This stock size is difficult to obtain, and it was decided that it would be more cost effective and a better use of time to use the 3 inch Aluminum stock on hand rather than purchasing a new block of material.

Prior to manufacturing, the upright underwent over 65 design edit processes. The overall design was consistently updated to account for the caster angle, the overall thickness of the part, the Ackerman geometry when connecting the tie rods, and the applied forces acting from the bottom contact patch of the tire. During Finite Element Analysis of the upright design, the forces acting on the bottom contact patch of the tire were translated up to the points of the attachment on the upright, as seen in *Figure 62*.

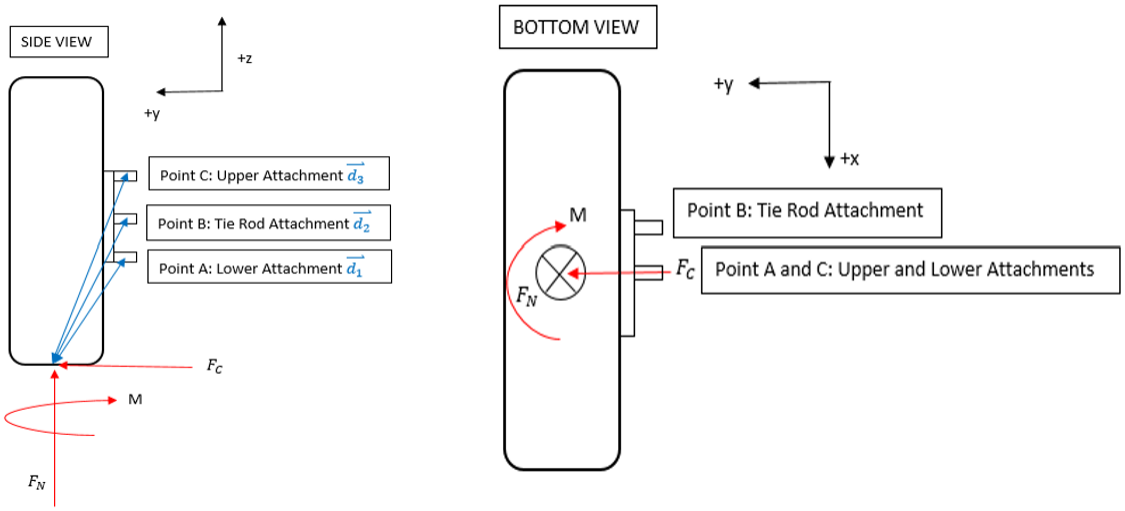

Figure 62: Contact patch forces and their translation to the upright attachments

The figures above represent the forces acting upon one tire during the most influential moments of steering where the variables F_C, F_N, and M represent the centripetal force, the normal force, and the maximum moment at the center point of the contact patch. These forces were calculated using the following equations:

$$\mathrm{F}_C = \frac{\mathrm{mV}^2}{\rho} \tag{8}$$

$$\mathrm{F}_N = \mathrm{mg} \tag{9}$$

$$M = 2F_N \mathrm{d} \tag{10}$$

The variables m, V, ρ represent the vehicles mass, velocity around the minimum radius of curvature, and the minimum radius of curvature, respectively.

These forces were then translated up to the points of interest on the upright using the Vector Method. The total forces acting at each desired point were determined by the sum of the total forces at the contact patch, applied in the opposite direction.

$$\mathrm{F}_{\mathrm{Total}} = \Sigma - \mathrm{F}_1 + \mathrm{F}_2 + \cdots \mathrm{F}_{\mathrm{N}} = -(\mathrm{F}_{\mathrm{C}} + \mathrm{F}_{\mathrm{N}}) \tag{11}$$

The total amount of forces acting on each attachment point was the same. Likewise, the total moment applied to the points of interest was calculated using the sum of each force acting at the contact patch cross multiplied with the distance to the point of interest in addition to the moment already acting upon the knuckle when the vehicle is traveling downhill, braking, and turning at the same time.

Endeavour Frame

The Denver Endeavour frame sub-team sought to reduce the torsion in the frame across the entire rover, make the rear seat more comfortable for the rider, and ensure the rover fits into a 5ft x 5ft x 5ft cube. In order to accomplish these goals, an additional folding mechanism was designed, frame adhesion was considered, and a seat support bracket was improved.

Hinge Design

In order to ensure the rover would fit in the competition-specified volume constraint, the frame team created a hinge for the front pedals. The initial idea would have a hinge locking system to raise pedals on the front side that would collapse onto itself, making the overall length of the rover around 10 inches shorter in order to accommodate the 5ft x 5ft x 5ft cube. *Figures 63* and *64***,** demonstrate the collapse mechanism that will be used to meet the compact size requirement during competition.

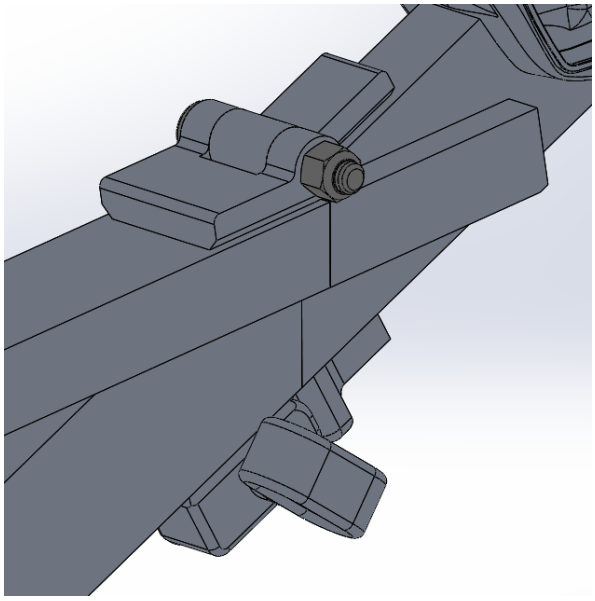

Figure 63: SolidWorks rendering of the front arm hinge design, folded

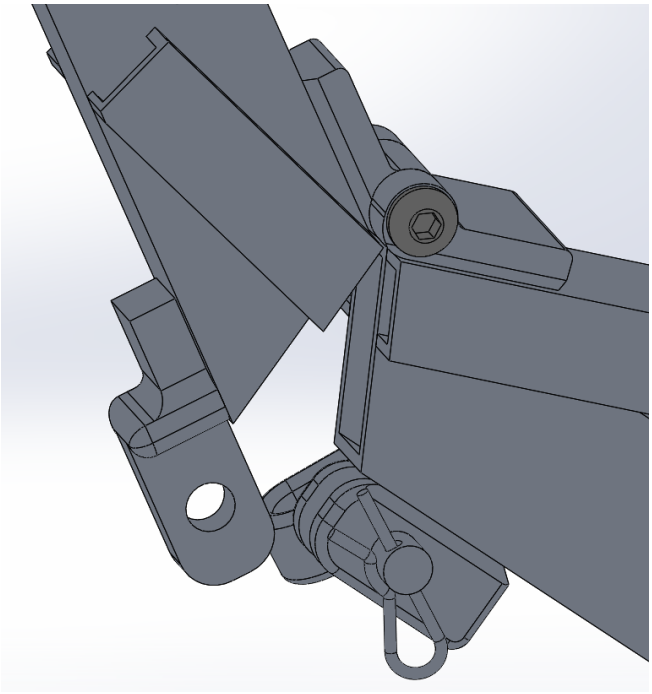

Figure 64: SolidWorks rendering of the front post hinge design, extended

Two years ago, an attempt was made during competition to pass this test, but the requirements were not met because pedal box extended passed the constrained sizing. This year's plan is to meet this requirement by utilizing this folding mechanism, and be able to fold

and unfold, it quickly and efficiently. This design has a bottom locking mechanism that is in double shear, which will withstand the rider's force, as well as, fix the pedal box in place during competition. This mechanism is locked in place using a pin, with a handle that will make for easy installation and removal. A safety cotter pin will ensure that the locking pin is stable within the locking mechanism and that it does not fall out during competition. The hinge on top of the collapsing mechanism ensures smooth rotation of the pedal box post and has a nut and bolt keeping it together. *Figure 65* shows the FEA done on the hinge. As seen in the figure, the force applied to the pedal box holder does not translate to the added parts. Forces, such as gravity and torsional forces, were used to simulate pedaling from the rider. The forces that were used for calculations exceeded actual expected values by 50 lbf at each bolt due to the gear pedal box receiving all the applied forces. Additional FEA, and hand calculations, might need to be done to make sure the geometries of the pins and bolt have a safety factor greater than two. *Figure 66* shows the free body diagram of the forces and moments acting on the hinge.

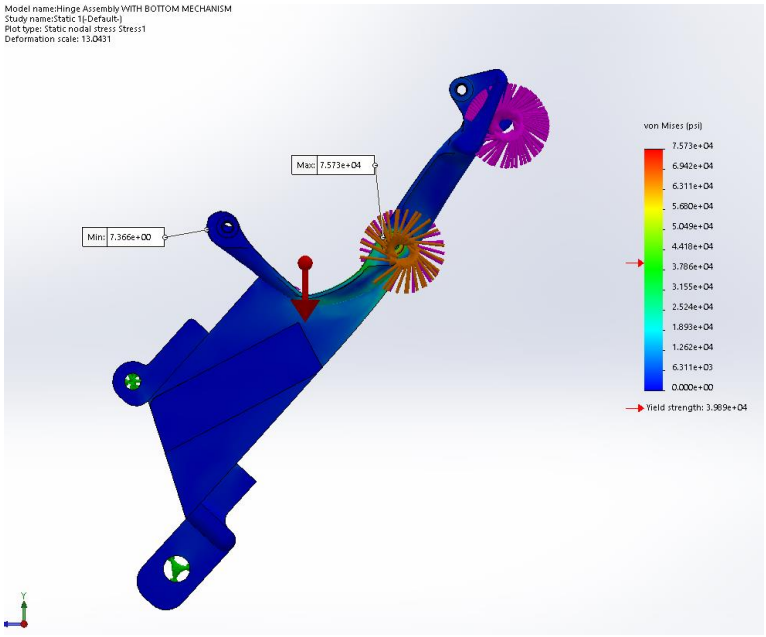

Figure 65: SolidWorks FEA analysis of the pedal box

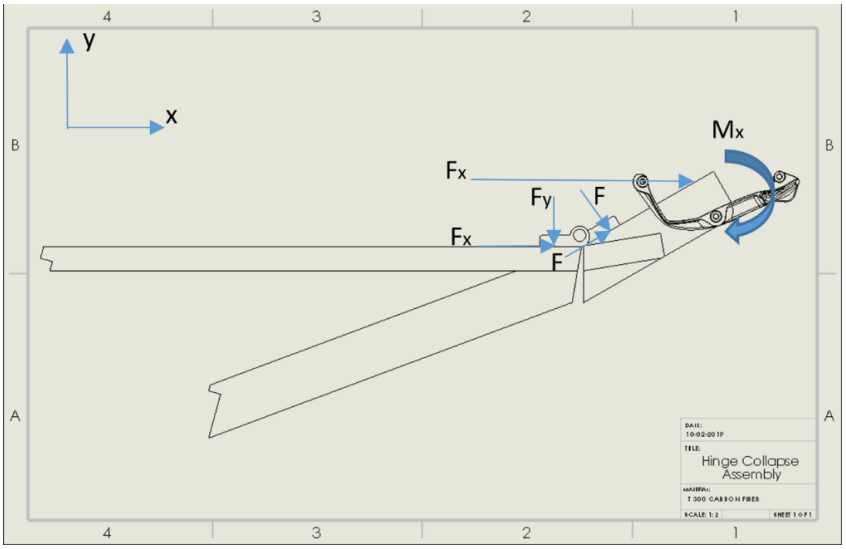

Figure 66: Free body diagram of the front post hinge

Design adjustments were made to the bottom locking mechanism including adding tolerances and changing design as could be compared in *Figure 67*.

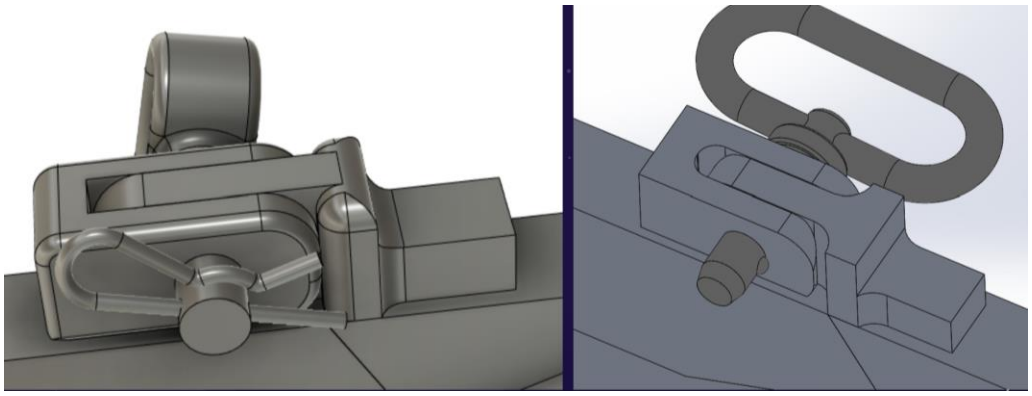

Figure 67: Old design of hinge, seen on left. New design of hinge, seen on right

The HAAS TM2 was used to machine all four parts from 6061-T6 Aluminum stock. Tabs were used to keep parts attached to the stock that was being held by clamps. A ½-inch flat end mill was used to cut the parts. The finished parts could be seen in *Figures 68* and *69,* below. The finished parts include the handle and shoulder bolt in them.

Figure 68: Finished release mechanism for the hinge, including the release pin handle

Figure 69: Upper hinge components with shoulder bolt

Seat Support Bracket Design

An additional element that the frame team decided to remanufacture, with a completely new design, was the seat support which is placed between the upper portion of the seats. The purpose of this bracket is to keep the seats from bumping into each other or shifting during the competition, as well as maintain frame rigidity along the entirety of the rover. The reason for redesigning this part was because on the original design no analysis was run on the piece and it ended up cracking from stress and torsion, as seen in *Figure 70*. The initial design of the seat support featured a crossed "X" section in the middle, shown in *Figure 71*, below.

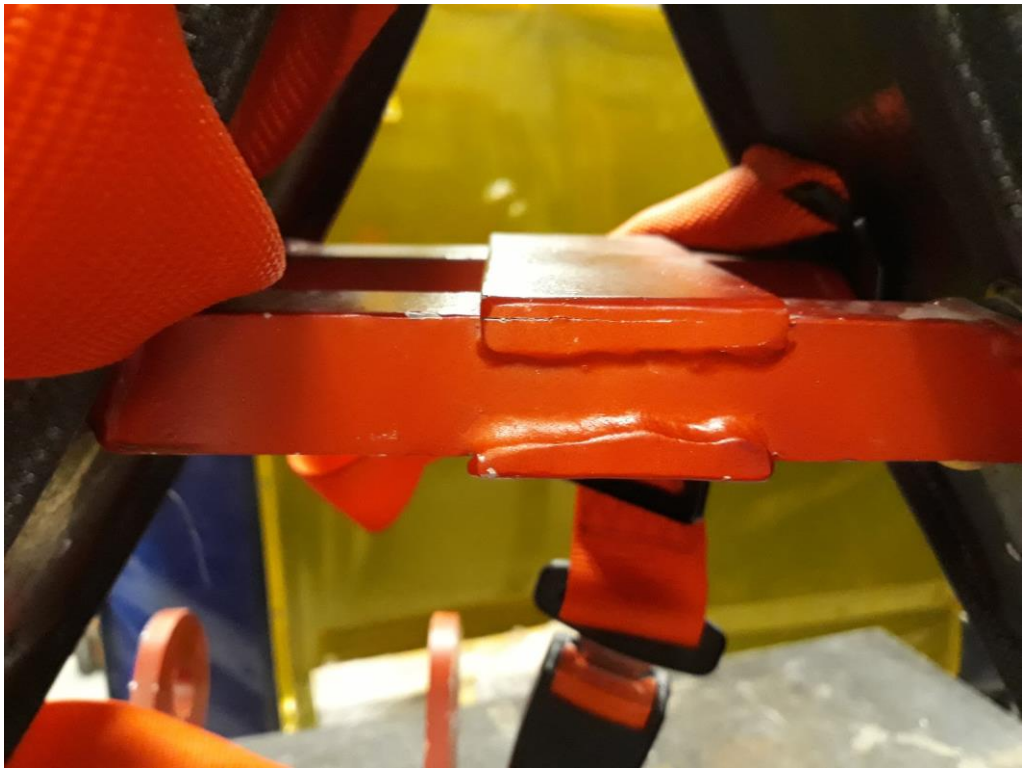

Figure 70: Visible crack in welds on seat support bracket

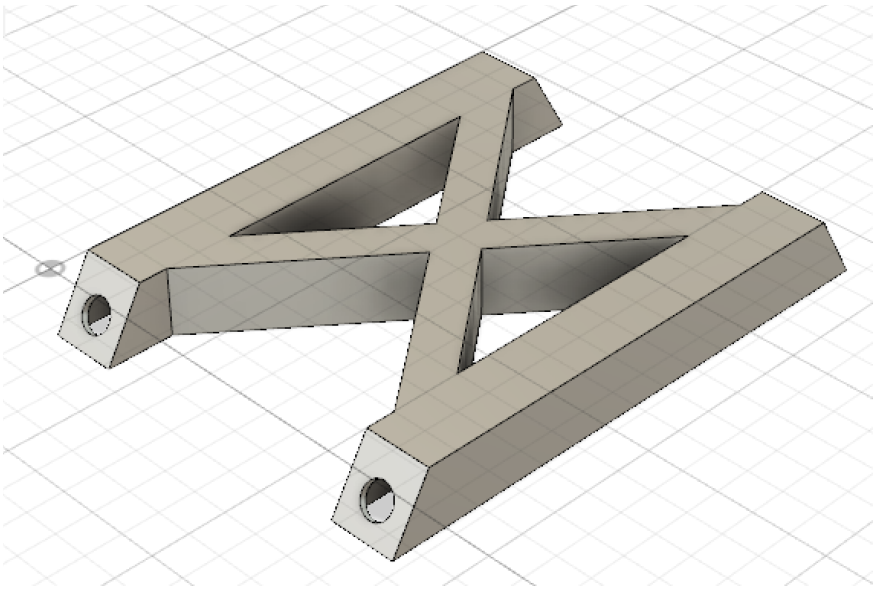

Figure 71: "X" Design seat support

The finite element analysis ran on this part was done by applying twice the amount of force acting back on the seats, by the riders, on all four points of connection on the seat support

where the support is bolted into the seat. This analysis yielded a safety factor of 1.572. After deliberating with the rest of the team, we found that due to all the sharp corners on the inside of the part, it would be hard to manufacture to the right dimensions, as well as some design flaws such as setting the bolt holes too far apart; this lead to a decision to come up with a new design.

The new design on the seat support is shown in *Figure 72*, which has an “H” shape in comparison to the first “X” design.

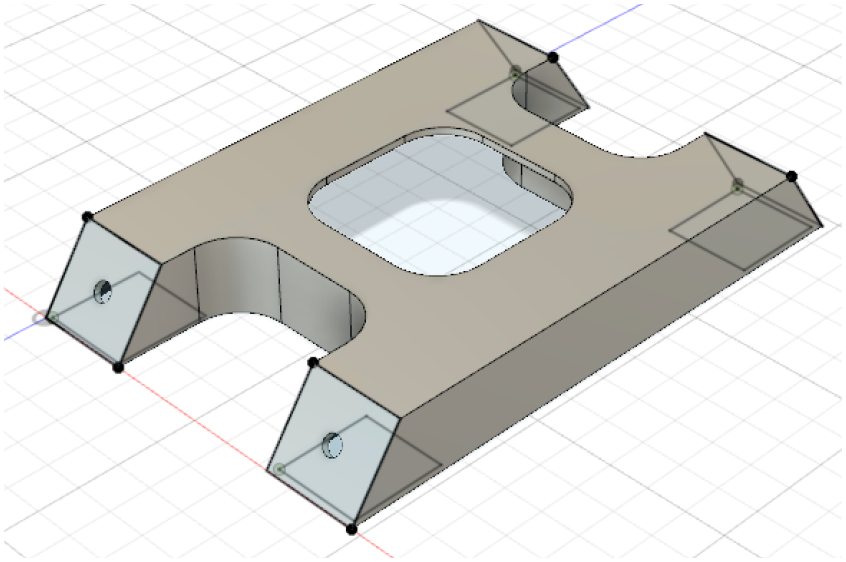

Figure 72: "H" Design seat support

This new “H” design is significantly lighter than the first design, as the first design was 10.854 ounces and the new design is 7.094 ounces. Running finite element analysis was done on the new design by assuming the rover would be rotating while the riders turn, causing torsion between the front and back seats; assuming two stationary points where the bolts would be while placing twice the amount of force the riders would be placing on the seats on the other, opposing two points (*Figure 73*). The FEA yielded a safety factor of 5.071.

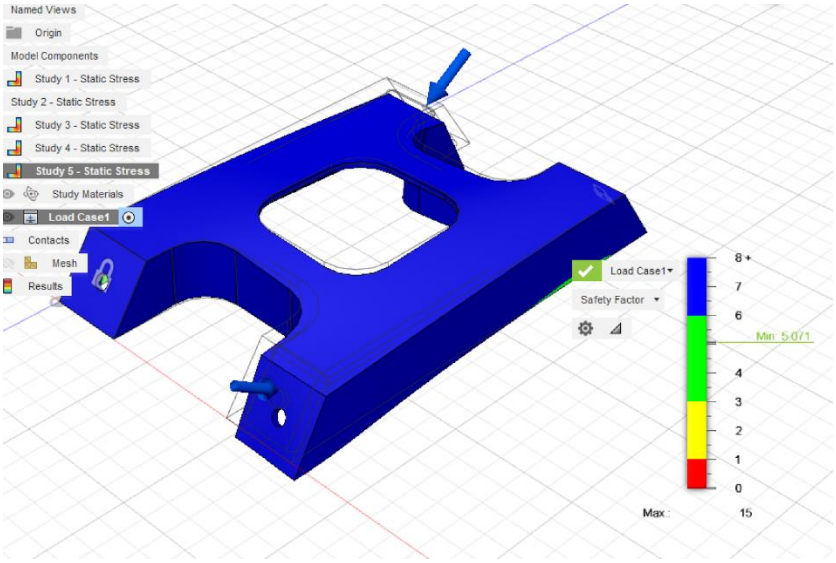

Figure 73: FEA results for "H" shape seat support

This part has dimensions of 7.125in x 4.875in x 1.00in; in order to get a part with those dimensions while being able to machine both sides, a 10.00in x 6.00in x 1.125in piece of aluminum 6061-T6 sheet was cut. The part was machined on a CNC mill using two endmills, a ½-inch flat endmill for the major shaving and a ¼ in ball endmill for more precise grooves on the inside, as well as, contouring the outside. Before machining the stock, the faces needed to be squared off so that when it's placed in the vice, it accurately cut the desired piece out. Squaring the faces was done by placing the stock long side up in the vice and using the ½ in flat endmill that we were already planning on using for the part to shave off 0.100in off the first side, then flipping it, and then shaving 0.100in off the other side. Then the part was clamped into the vice by the newly squared sides and the program was run.

The top section was manufactured first by finding the center point that was anointed in Fusion 360 by touching off the x-plane, y-plane, and z-plane, and then offsetting the x-plane by 1.125 in and the y-plane by 0.625 in so that the part will be machined from the center of the stock and the outside can be scrapped. When the top part was complete, the entire part was removed from the vice and the remaining edges were broken off by hand. It was found that the 1.00in stock was not really 1.00in, it was a little bigger than what was printed on it, which is probably so that it can be stored easily. When the part was flipped, the bottom had to be machined manually in order to shave off the excess aluminum, as well as, get the middle part out of the stock. Manufacturing the entire part, including cleaning, sanding, and buffing, took around 5 hours.

Frame Adhesion

This year a design modification included adhesion of all components, that will be attached to stingers, by Hysol EA 9309NA instead of bolting them on the stringers. The reason for such modification was the consideration of structural strength of stringers and its decrease due to boring through the carbon fiber stringers. Torsional testing was conducted to determine the strength of the adhesive bond, and to determine if it could withstand the torsional stresses that occurred during the competition two years ago. A torque wrench was be used to simulate stresses within the adhesive connection. The components that stress was applied to, included a piece of stringer without any bolt holes and a piece of last year's steering design that wasn't used this year. The steering component needed to have slot for the torsion wrench, as seen in *Figure 74.* This square slot was cut on the wire EDM and the setup for the cut seen in *Figure 75*.

Figure 74: Slot cut into steering component in order to place torque wrench for proper testing

Figure 75: Wire EDM set up used to cut square slot into aluminum component

The aluminum components, for the entire rover, will be bolted to each other and then, adhered to the stinger as could be seen on *Figure 76*.

Figure 76: Aluminum components bolted to each other, then adhered to the carbon fiber stringer

To bind aluminum collar and possible bulkhead to a stinger, a mixture of Hysol EA 9309 NA needed to be prepared. This procedure included weighing two parts of 100 to 23 of Hysol that include Epoxy Paste Adhesive (Part A) and red curing agent (Part B), respectively. Mixing needs to be thorough, with no air bubbles present in the mixture. The paste had to have an even, light pink color, when done mixing. Application of the pink paste to both the aluminum parts, and area where bulkhead and collar connect, is required. When sliding components on to stringer, air bubbles between components were prevented by rotating components. Before letting Hysol dry, components needed to be in desired position and angle and any excess paste needed to be cleaned around the parts. The final desired bonding can be seen in *Figure 77.*

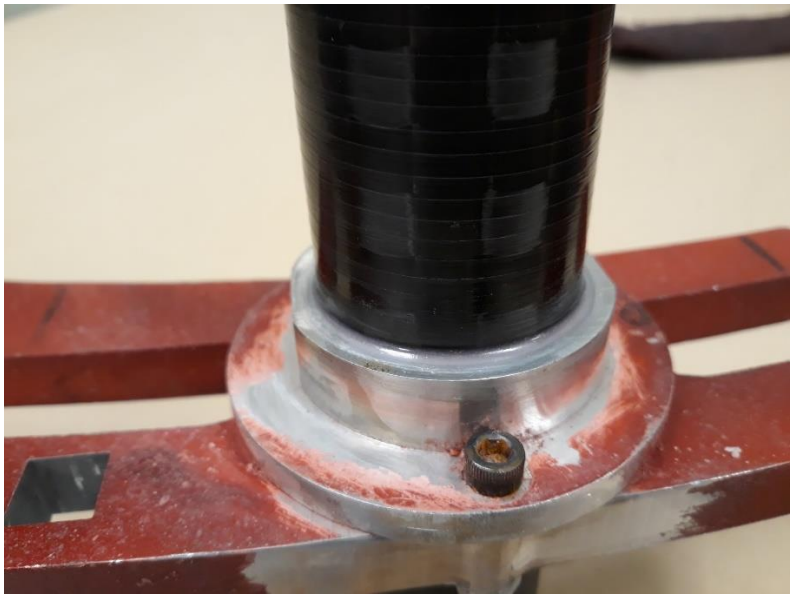

Figure 77: Desired thickness and outcome of prepped bond

Curing the resin at room temperature took one to two days. The final step before testing the adhesive, was to completely cure it by heating all the parts of the assembly to 150 degrees Fahrenheit and keeping it at this temperature for two hours. After conducting testing, it was determined that the Hysol resin would successfully stiffen the frame and the torsion along the frame would not be enough to break the bond of the resin.

Budget and Cost

The total estimated budget for the Denver Endeavour team is $11,837. The largest expense for our team was travel. We were to be travelling 19 hours from Denver, Colorado to Huntsville, Alabama, via rental van. We also accounted for lodging and food for our 8 team members. We planned to optimize our expenses for travel by sharing a van that seats all team members and sharing hotel rooms along the way, to reduce the number of reservations that need to be made. The wheels team budget is around $2,495 and the largest expense for the wheels is the cost of carbon fiber needed for the layups. The frame sub-team is estimating $2,150 for the completion of their parts and, much like the wheel team, the greatest expense for the frame team is carbon fiber for the torsion plate and the prefabricated stringers. Suspension and steering components will be mostly made of aluminum and the budget for this sub-team is much less than the other teams. The total budget for the steering and suspension sub-team is $1,432 for the design. A complete breakdown of the estimated budget for the Endeavour designs can be found in *Appendix A.* In addition, an updated budget from the spring semester is found in *Appendix J.*

Fundraising/Sponsorships

Our team created a crowd-funding page through Milo's Crowd and the Office of Advancement. So far, the Endeavour team has gained a generous $1,000 sponsorship from Torch Technologies, in addition to raising a total of $435 towards our budget goals using the crowdfunding. Torch Technologies is a defense company located in Huntsville, Alabama and our team updated them regarding the progress we were making on the Endeavour and included their

logo on our final design, and team shirts. In addition to Torch, Rock West Composites has graciously assisted us with our project by providing us with a 15% discount for the purchase of our 4 carbon fiber stringers. Rock West had asked to be updated throughout the manufacturing process, as well as, competition. EMJ has generously donated some of our 6061-T6 aluminum stock to our team, saving money from our budget.

Gantt Diagrams

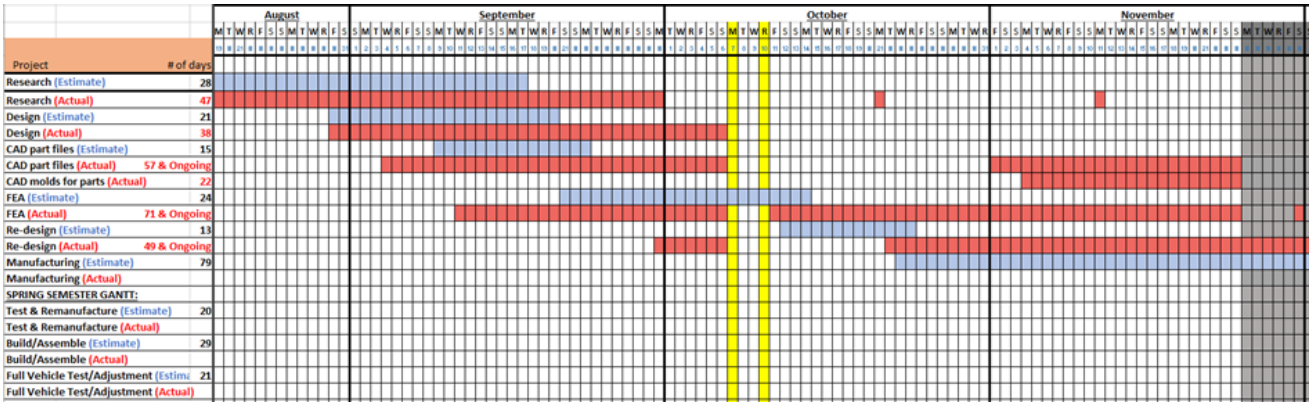

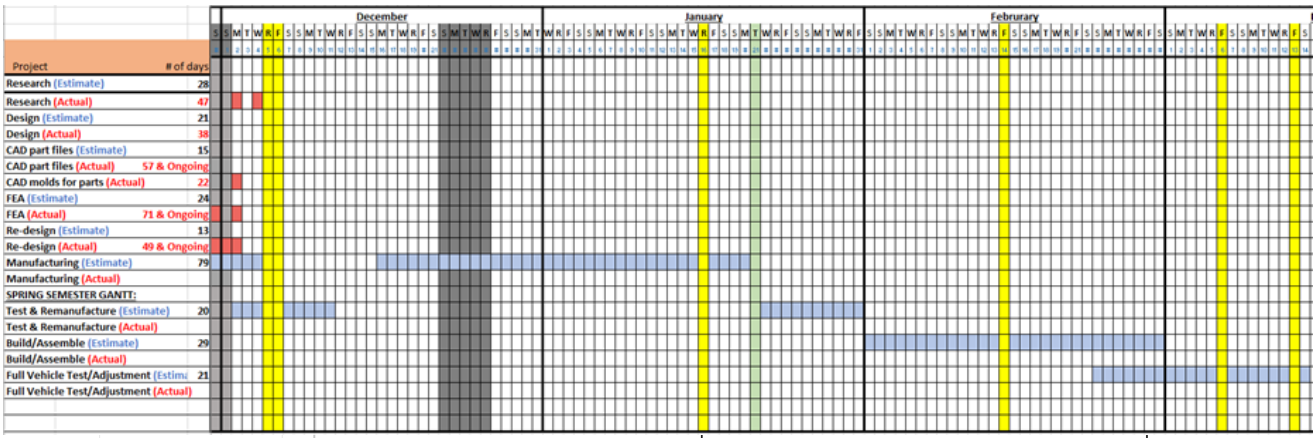

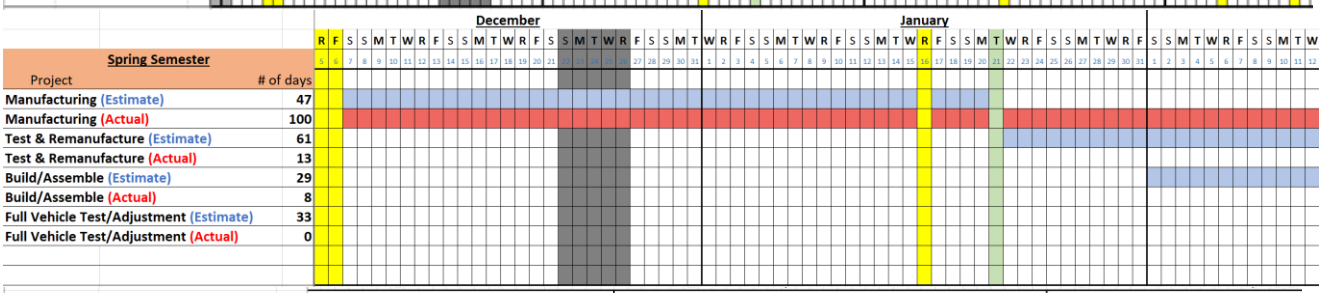

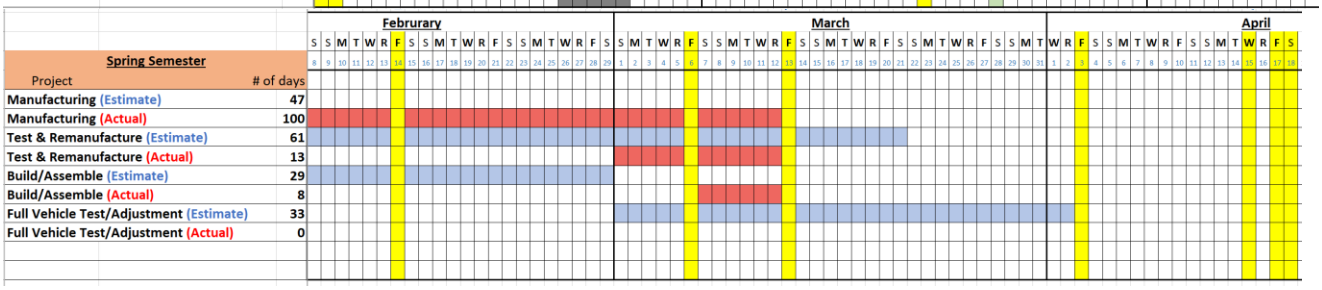

References

Epiphany Rover Team 2016-2017

Odyssey Rover Team 2017-2018

Red Rover Team 2018-2019

Professor Joseph Cullen

Professor Doug Gallagher

Professor Dr. Dana Carpenter

Professor Dr. Ronald Rorrer

Composites Expert Kevin Fornall

FSAE Team Lead Nicholas Lanzoni

Odyssey Team Lead Ryan McCort

Don and Vi O'Connor - Any and All Bikes, Denver, CO

Bright Hub Engineering, 12 Nov. 2018, www.brighthubengineering.com/machine-design/12903-exact-straight-line-mechanisms/.

Gabrian. (2019). 6061 Aluminum: Get to Know its Properties and Uses. Retrieved from Gabrian: https://www.gabrian.com/6061-aluminum-properties/

Gillespie, Thomas D. *Fundamentals of Vehicle Dynamics*. 400 Common Wealth Drive Warrendale, PA 15096-0001: Society of Automotive Engineers, Inc., n.d. Textbook.

Juvinall, R. C. (2012). Fundamentals of Machine Component Design. Hoboken: John Wiley & Sons, Inc.

J.Y. Wong, Ph.D., D.Sc., F.I.Mech.E, F.A.S.M., F.C.S.M.E. *Theory of Ground Vehicles*. 605 Third Avenue, New York, NY: John Wiley & Sons, Inc., 2001. Textbook.

Occupational Safety and Health Administration. "Materials Handling: Pushing, Pulling, and Carrying." *United States Department of Labor* (2019).

Safety, Canadian Centre for Occupational Health and. "Pushing and Pulling- General ." *OSH Answers Fact Sheets* (2019).

Tutorials, E. (2013, March 15). Steering Mechanisms: Kinematics of Machines Tutorials. Retrieved from Engineering Tutorials: http://engineering.myindialist.com/2013/steering-mechanisms-kinematics-of-machines-tutorials/#.XZjrp3dFyM8

Appendices

Appendix A: Estimated Budgets

Travel	Quantity	Cost	Total Cost
Hotel	4 rooms, 8 nights	$100 ea	$ 3,200.00
Rental Van	1 van, 10 days	$200	$ 2,000.00
Gas	2600 miles, 15 mpg	$3	$ 520.00
Food	8 people, 2x daily	$10/meal	$ 1,600.00
		Total:	$ 7,320

Wheels	Quantity	Cost	Total Cost
Aluminum (6061-T6)	2	$ 53.37	$ 106.74
Carbon Fiber Fabric (Toray T300)	20	$ 35.39	$ 707.80
Expanding Foam (FlexFoam-iT25)	3	$ 196.91	$ 590.73
Epoxy	2	$ 350.00	$ 700.00
Polyurethane rubber (Simpact 60A)	3	$ 129.87	$ 389.61
		Total:	$ 2,494.88

Frame	Quantity	Cost	Total Cost
Carbon Fiber Stringers	4	$ 484.00	$ 1,936.00
Carbon Fiber Fabric (Toray T300)	5 yards	$ 50.00	$ 250.00
Resin and Epoxy	1	$ 40.00	$ 40.00
2"x2" Aluminum Stock	4	$ 20.00	$ 80.00
2"x1"x48" Aluminum Stock	1	$ 24.00	$ 24.00
		Total:	$ 2,330

Suspension and Steering	Quantity	Cost	Total Cost
Aluminum (6061-T6)	Various dimensions	Varies	$ 1,200.60
Threaded End Pins	10	$ 1.80	$ 18.00
Mini Bearings	32	$ 8.99	$ 35.96
Handle Bearing	6	$ 24.62	$ 147.72
PLA Roll	1	$ 24.99	$ 24.99
JB Weld	1	$ 4.88	$ 4.88
		Total:	$ 1,432.15

Appendix B: Steering Angle Calculations

L	82	in (6ft 10in)	
R	180	in (15ft)	
t	44	in	
δ_o		δi	
RAD	DEG	RAD	DEG
0.385617	22.09423	0.478722	27.42874

Appendix C: Steering Force Calculations

Caster Angle φ	2	DEG	0.034907	RAD
Tire Radius R	13.5	in	1.125	feet
Trail, a=φR	0.471238898	in		
Length from Rear to COG lR				
lR	33.2	in	*Guess of 40% L	
Length from Front to COG lF				
lF	49.8	in	*Guess of 60% L	
Total Length Center of Back tire to Center of Front Tire				
L	83	in (6ft 10 in)		
Fy Calculations				
$Fy,f = (lR/L)m(V^2/R)$				
Weight of Riders + Vehicle				
W	430	lbf		
Mass				
m	13.36649052	lbm		
V	10	mph		
V	14.66666667	ft/s		
Fy	1022.322001	lbf		
Fyy Calculations				
Length in x axis from center of Front Tire to end of Knuckle attatchment				
lK	4	in		
F = (a/lk)Fy	120.4394733	lbf		
F_{ts} =	124.4991014	lbf		
F_{handle} =	26.28198019	lbf		

Appendix D: Hoop Stress m-file

```
% Hoop Stress


% Calculates minimum circumferential surface thickness assuming:
% 512lb load, only one tire in contact with the ground
% 27" diameter * 4" thickness
% Models wheel like thin walled pressure vessel
% For thin wall assumptions to be valid the diameter/thickness > 20 must be
% the case.
%
% 7000psi UTS for CFRP
load = 512; % pounds
D = 27;     % inches - wheel diameter
w = 4;      % inches - wheel thickness
UTS = 7000; % lowest value for CFRP UTS found on MATWEB
Pressure = load / (D*w);
t = (Pressure *D) / (4*UTS)
```

Appendix E: Sidewall Thickness m-file

```
% Sidewall Thickness Required


% Solves required sidewall thickness
% Assumptions:
% The load of the vehicle, transmitted to the wheel through the wheel hub is
% supported by CFRP in tension only. Integrating thickness*sin(O) from 0 to pi,
% this means the cross-sectional area of CFRP supporting the load is 2*thickness.
% Research gives UTS values for CFRP 487 - 825MPa, but yield strength
% ranging from 945 - 1080 MPa. Using the lowest value available, 487MPa
% roughly equals 7000psi
% If stress = force over area, area = force over stress. Area equals 2t.
% t = Force / (2*stress). Although there are two sidewalls, we&#39;ll use a
% safety factor of two, and NOT make the equation t = F / (4 stress)
% Assume vehicle weight is 512 pounds, and only one wheel is in contact with
% the ground
P = 512; % pounds
Stress = 7000; % psi
t = P / (2* Stress)


% Above was for a vertical sidewall
% Since Endeavour sidewall is at a slight angle, we must use trig to calculate the
% forces in the sidewall


dx = .5;    % length of the inset of the angled bit
dy1 = 9.9;  % height of the angled bit
dy2 = 9.78; % height of the slightly shorter side angled bit
theta1 = atan (dx/dy1);
theta1d = theta1*180/pi % angle of endeavour sidewall degrees
theta2 = atan (dx/dy2);
theta2d = (180/pi)* theta2 %angle of endeavour sidewall degrees
p_1 = P/cos(theta1) % force along the hypotenuse
p_2 = P/cos(theta2) % force along the hypotenuse on the other side


format long;
t1 = p_1/(2*Stress)
t2 = p_2/(2*Stress)
```

Appendix F: Bending at Hub m-file

```
% Bending at Hub


v = 15;         % enter speed in mph
W = 512;        % weight of vehicle and drivers lbf
r = 17;         % turning radius
Sy = 255000;    % Tensile strength of material in psi
n = 2;          % safety factor
v = v*5280/3600; % puts speed into ft/s
m = W/32.2;     % converts weight in pounds into mass in slugs
a = v^2 / r;    % radial acceleration
F = m*a;        % sideward force exerted in the tire
t = .048;
b = 12.4;
w = 4;
I = (1/12)*b*w^3 - (1/12)*(b-2*t)*(w-2*t)^3;
M = F*b;
sigma = (M*(w/2))/I;
SF = Sy/sigma;
```

Appendix G: Rock West Composites 14029-D data sheet

Rock West COMPOSITES

14029-D

Intermediate Modulus Unidirectional Prepreg

Product Description

Rock West Composites PROPreg™ is a heat activated carbon fiber + epoxy system recommended especially for fiber-reinforced composite parts. This prepreg exhibits excellent mechanical strength and stiffness properties.

Handling, Safety and Storage

- Gloves and safety glasses are recommended for user's personal protection.
- When removing from freezer keep sealed until fully thawed.

Material Specification (Composite)

Physical Properties	
Fiber	T800S
Resin	250F Epoxy
Shelf Life (°C/°F)	6+ months (@ ≤-18°C / 0°F) 1 month (@ 20°C / 68°F)
Gel Time @ 135°C / 270°F	3 – 6 minutes
Tg Glass Transition (°C / °F)	130 ± 10 °C / 266 ± 18 °F

Typical Composite Mechanical Properties (0° orientation) @ 23 °C		
Tensile Strength (MPa)	2950	ASTM D 3039
Tensile Modulus (GPa)	154	
Comp. Strength (MPa)		
Comp. Modulus (GPa)		
Flexural Strength (MPa)		
Flexural Modulus (GPa)		

Processing

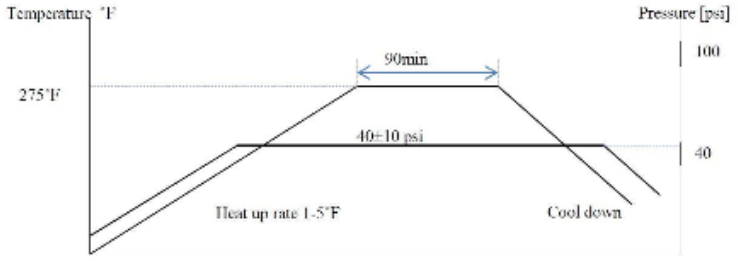

- Pressure required for adequate consolidation
- Heat up (ramp) rate is listed as an acceptable range, in degrees F per minute
- Laminates cure for 90 min. @ 275 °F or longer at lower temperatures

Manufacturing: 3392 West 8600 South, West Jordan, UT 84088 | Corporate: 1602 Precision Park Lane, San Diego, CA 92173
Ph: 801.566.3402 | Fx: 855.301.9874 | www.rockwestcomposites.com

Appendix H: McMaster-Carr Stock Ordered Parts

Manufacturer	**Part Name**	**Part Number**	**Size**	**Qty.**	**Total Cost**
McMaster-Carr	Super-Swivel Ball Joint	6960t610	⅜” - 24 Thread: Male	4	$42.72
	Connecting Rod: Internally Threaded	6516K62	⅜”-24 Thread: Female, 12” Length	2	$30.78
	18-8 Stainless Steel Shoulder Screw	90298A798	⅝ “ Shoulder Diameter 1.5”-13 Thread 1.5” Shoulder Length	6	$100.74
	Medium Strength Steel Locknut	9719A025	½” -13 Thread: Use with Cotter Pin Lock	6 or 1 pack of 10	$4.74
	1004-1045 Carbon Steel Cotter Pins	90520A101	1/16 “ Diameter, ¾” long	6 or 1 small pack of 100	$2.13
	18-8 Stainless Steel Washers	92141A034	0.578” ID and 1.062”OD	20 or 1 pack of 50	$6.18

Appendix I: Braking on 30-degree Incline Calculation of Forces at Wheel

```
%% This will attempt to look at the braking calculations of the Rover going
%% down a hill and stopping at 3.4 m/s^2, the standard in Road Vehicle Tech


%% Inputs


W = 512;    % Weight of Rover + Riders in lb
L = 85;     % Length of Wheelbase in inches
l1 = 40;    % Distance to CG from front wheels in. inches
r_r = 85;   % Rotor radius in mm
r_w = 13.75;   % Wheel radius in inches
angle = 30; % angle of ramp in deg
h = 10;     % height of CG from ground in inches
mu = 1;   % Coeffecient of Static Friction between road and tire surfaces


%% Calculations
l2 = L-l1;              % distance from rear wheel to CG
angle = angle*pi/180;  % convert angle to radians
r_r = r_r/(25.4*12);      % convert rotor radius to feet
r_w = r_w/12;             % convert wheel radius to feet
Fn_f = (W*cos(angle)*l2+W*sin(angle)*h)/L; % Normal Forces on Front Wheels Combined
Fn_each_f = Fn_f/2;       % Normal Force on each front wheel
Fn_r = W*cos(angle)-Fn_f; % Normal Force on rear wheel
sumF_n = Fn_f+Fn_r ;      % Total Normal Force on all wheels
Fb_max_f = 2*mu*Fn_f; % Maximum Braking force that could be applied to front wheels
Fb_max_f_each = Fb_max_f/2; % " " to each front wheel
Fb_max_r = mu*Fn_r;     % Maximum Braking force to rear wheel
T_front = Fb_max_f_each*r_w %Torque on each front wheel
T_rear = Fb_max_r*r_w % Torque on rear wheel
Fb_min = W*sin(angle)
```

Appendix J: Spring Semester Budget Update

Fall 2019		
Items purchased	**Total Cost**	**Updated Balance**
Starting Balance	$2,400.00	$2,400.00
MDF Board x 6	-$187.02	$2,212.98
Carbon Fiber Stringers x4	-$918.80	$1,294.18
MISC Home Depot (Maddie Reimbu	-$122.87	$1,171.31
MISC Home Depot (Kolton Reimbur	-$67.40	$1,103.91
Locktite Red Epoxy Adhesive	-$152.56	$951.35
Fundraising		$ 1,425.00
Items purchased	**Total Cost**	**Updated Balance**
Student Funds Rollover (Spring)	$951.35	$2,376.35
Carbon Fiber Fabric	-$208.95	$2,167.40
Genuine Aircraft Hardware	-$28.05	$2,139.35
Aircraft Spruce Hardener	-$295.36	$1,843.99
McMaster Carr Hinge	-$17.59	$1,826.40
McMaster Carr Steering	-$124.25	$1,702.15
ReoFlex 60 Rubber	-$399.08	$1,303.07